We are IntechOpen, the world's leading publisher of Open Access books
Built by scientists, for scientists

6,900
Open access books available

185,000
International authors and editors

200M
Downloads

Our authors are among the

154
Countries delivered to

TOP 1%
most cited scientists

12.2%
Contributors from top 500 universities

CLARIVATE ANALYTICS
BOOK CITATION INDEX
INDEXED

WEB OF SCIENCE™

Selection of our books indexed in the Book Citation Index
in Web of Science™ Core Collection (BKCI)

Interested in publishing with us?
Contact book.department@intechopen.com

Numbers displayed above are based on latest data collected.
For more information visit www.intechopen.com

Climatic Effect of the Greenhouse Gases Clusterization

Alexander Y. Galashev

Institute of Industrial Ecology of the Ural Branch of the Russian Academy of Sciences
Russia

1. Introduction

The Earth's atmosphere is a complex dynamic system, which protects the biosphere. One of the significant factors impacting the Earth's radiation balance is the greenhouse effect. The ability of the atmosphere to capture and recycle energy emitted by the Earth's surface is the defining characteristic of the greenhouse effect. Greenhouse gases (GHG) dissipate heat in the atmosphere. The greenhouse effect is observed only when radiant heat stays in the troposphere, instead of leaving into Space. Layers lying above the troposphere, such as stratosphere and thermosphere, serve as an obstacle for heat loss into Space. At low temperatures, characteristic of stratosphere and the lower thermosphere, water clusters, capable of absorbing molecules of other gases are formed. Many chemical compounds present in Earth's atmosphere behave as greenhouse gases.

The fact that the Earth's climate is altered by a change in atmospheric composition is well known. The analyses of various paleorecords, such as ice cores, have shown that atmospheric composition and climate have been correlated over the past 100,000 years. Water Vapor is the most abundant greenhouse gas in the atmosphere. However, changes in its concentration is also considered to be a result of climate feedbacks related to the warming of the atmosphere rather than a direct result of industrialization. The feedback loop in which water is involved is critically important to projecting future climate change, but as yet is still fairly poorly measured and understood.

Carbon dioxide is a greenhouse gas, and the increased concentration of carbon dioxide in the atmosphere must influence earth's radiation balance. The rising concentration of atmospheric CO_2 in the last century is not consistent with supply from anthropogenic sources. Such anthropogenic sources account for less than 5% of the present atmosphere, compared to the major input/output from natural sources (~95%). Hence, anthropogenic CO_2 is too small to be a significant or relevant factor in the global warming process, particularly when comparing with the far more potent greenhouse gas water vapor. The rising atmospheric CO_2 is the outcome of rising temperature rather than vice versa. The time taken for atmospheric gases to adjust to changes in sources or sinks is known as the atmospheric lifetime of a gas. The atmospheric lifetime of carbon dioxide is estimated as 5-200 years (Essenhigh, 2009). An individual molecule of CO_2 has a short residence time in the atmosphere. However, in most cases when a molecule of CO_2 leaves the atmosphere it is simply swapping places with one in the ocean. The CO_2 molecules cannot accumulate in the atmosphere, because of Henry's Law, which says that most of the atmospheric CO_2 must be

exchanged with the ocean water. CO_2 is essentially chemically inert in the atmosphere and is only removed by biological uptake and by dissolving into the ocean. Dissolution of CO_2 into the oceans is fast but the transfer of carbon from surface waters to the deep ocean largely occurs by the slow ocean basin circulation and takes about 500-1000 years.

Methane is an extremely effective absorber of radiation, though its atmospheric concentration is less than CO_2 and its lifetime in the atmosphere is brief (10-12 years), compared to some other greenhouse gases (such as CO_2, N_2O). Concentrations of nitrous oxide also began to rise at the beginning of the industrial revolution and is understood to be produced by microbial processes in soil and water, including those reactions which occur in fertilizer containing nitrogen. Ultraviolet radiation and oxygen interact to form ozone in the stratosphere. Existing in a broad band, commonly called the ozone layer, a small fraction of this ozone naturally descends to the surface of the Earth. The potential radiative impact of the ozone change on the stratosphere–troposphere exchange was investigated in (Xie et al., 2008). This analysis shows that a 15% global O_3 decrease can cause a maximum cooling of 2.4 K in the stratosphere. Carbon monoxide (CO) is not considered a direct greenhouse gas, mostly because it does not absorb terrestrial thermal IR energy strongly enough. However, CO is able to modulate the production of methane and tropospheric ozone.

Water vapor and atmospheric gases, such as CO_2, N_2O, CH_4, and others, have a decisive influence on the formation of thermal radiation fields. However, according to the Le Chatelier principle, there are opposite compensating processes in the atmosphere. Clusterization of greenhouse gases can be considered as one of these processes. Water molecules bind easily to one another by forming hydrogen bond complexes – clusters. These weak interactions (approximately 0.21 eV) perturb the rovibronic and electronic states of individual molecules, and alter the spectroscopy of water vapor (Vaida et al., 2001). The possible involvement of water clusters in these processes has been proposed for a long time (Bignell et al., 1970; Lee et al., 1973; Coffey, 1977; Wolynes & Roberts, 1978; Carlon, 1979; Dias-Lalcaca et al., 1981). The abundance and the vibrational spectrum of the water dimer and trimer were evaluated both theoretically (Shillings et al., 2010) and in an experiment (Goss et al., 1999). The temperature contributions of the greenhouse gases of the Earth's atmosphere to the greenhouse effect are determined in (Barrett, 2005) according to their volume fraction. So for water vapor this contribution should make 37.4 K. However, correction of 13.4 K is necessary to take into account the effect of water evaporation. Therefore effectively the contribution of water vapor decreases to 24.0 K.

Nitrogen forms the following series of oxides that formally correspond to all possible oxidation states from +1 to +5: N_2O, NO, N_2O_3, NO_2, N_2O_5; however, only two of them, nitrogen(II) oxide and nitrogen(IV) oxide, are stable under ordinary conditions and actively participate in the natural and industrial nitrogen cycles. Nitrogen oxides (NO_x) are of great importance for many atmospheric reactions. NO_3, radical is the most reactive of them; it is formed in the dark and is regulated by the chemical reactions occurring in the night atmosphere. When interacting with water, nitrogen oxides form nitric acid (HNO_3), which is not only the main component of acid rain, but also governs the main process of removing nitrogen oxides from atmosphere. Nitric acid plays the key role in the chemistry of polar stratosphere. It is involved in the formation of ozone holes. Nitrogen oxides directly participate in the formation and decomposition of the tropospheric ozone. Under the action of sunlight, nitrogen dioxide is transformed into monoxide NO, which, in turn, forms NO_2 by interacting with oxygen. Ozone and peroxide radicals are also involved in this cycle.

More carbon monoxide is emitted to the atmosphere every year than any other pollutant except for CO_2, and the amount of emitted CO increases every year. However, the data on the rise of CO concentration in the troposphere are quite contradictory. The results of measurements of CO content in samples of Arctic and Antarctic ice indicate that its concentration hardly varied for centuries (Platt & Stutz, 2008). There exist at least five varieties of CO, namely, two varieties with light oxygen (O_{16}) and three varieties with heavy oxygen (O_{18}). The first two varieties of CO may form directly in the atmosphere the year round. The much less common varieties of CO enriched with O_{18} are seasonal. Carbon monoxide is liberated from the ocean surface, similar to methane. Depending on the concentration of CO, the soil may be both the source and the sink of this gas. The main anthropogenic source of CO is the incomplete combustion of hydrocarbon fuel, including automobile fuel. The resident time of CO in the troposphere is from 0.1 to 0.2 year. As a result of the effect of hydroxyl, CO oxidizes to carbon dioxide. Because of the existing transverse gradient of CO concentration in the troposphere, the stratosphere serves as the sink of carbon monoxide. Monoxide NO stands out from among nitrogen oxides; its resident time in the troposphere is approximately one hundred years. At present, its concentration in the atmosphere increases by 0.25% a year. The transition of NO to the stratosphere causes a reduction of stratospheric ozone: nitrogen monoxide reacts with ozone to form nitrogen dioxide and oxygen.

The study of the properties of clusters is usually considered as a way of investigating the transition from gas to condensed liquid. In the case of water clusters, it is also possible to estimate the effect of hydration on the dynamics of chemical reactions in a regulated form. For example, the reaction between SO_3 and water vapor consisting of both monomers and clusters is extremely important from the standpoint of heterogeneous atmospheric chemistry (Akhmatskaya, et al., 1997), as it represents the final stage in SO_2 tropospheric oxidation, which eventually leads to the formation of sulfuric acid aerosols and acid rains. These reactions also result in the depletion of ozone, thus weakening the absorption of incident solar radiation and influencing the Earth's climate.

Atomic oxygen plays an important part in the formation of atmospheric ozone. Oxygen atoms formed in the dissociation of an O_2 molecule either associate again in the presence of another particle M necessary to withdraw the energy from a formed molecule according to the equation

$$O + O + M \rightarrow O_2 + M, \tag{1}$$

or interact with an O_2 molecule also in the presence of another particle and form an ozone molecule as follows:

$$O_2 + O + M \rightarrow O_3 + M. \tag{2}$$

Physically, an ozone molecule is stable, but the decomposition rate of gaseous ozone grows appreciably with an increase in the temperature and amounts of some gases, for example, NO, Cl_2, Br_2 and I_2, and also under the action of different radiations and particle fluxes.

The autoregulation of the atmosphere composition is due to the formation of water clusters and their subsequent capture of greenhouse gas molecules is, as a rule, ignored in the estimation of the Earth's radiation balance. The characteristics of infrared (IR) radiation absorption by water clusters incorporating molecules of the most abundant atmospheric gases – nitrogen, oxygen, and argon – were studied in (Galashev et al., 2005; Novruzova et al., 2007a, 2007b; Novruzova & Galashev, 2008).

The objective of this study is to investigate the absorption of different greenhouse gases by ultradisperse water medium with determining the spectra of infrared (IR) absorption and emission by $(H_2O)_n$ and $X_i(H_2O)_n$ (where X= CO_2, N_2O, CH_4, C_2H_2, C_2H_6, NO_2, NO, CO and O_3) systems under conditions typical of the troposphere. Also, in the light of the molecular dynamics calculations, the impact of atmospheric gases' clustering on greenhouse effect is examined.

2. Computer model

This work deals with the molecular dynamics study of the influence of clusterization of H_2O vapor and atmospheric gases such as CO_2, N_2O, CH_4, C_2H_2, C_2H_6, NO_2, NO, CO and O_3 on the greenhouse effect. The IR absorption spectra were calculated for systems formed by water clusters and molecules of the above greenhouse gases at 233 K. Due to clusterization a homogeneous single-phase system represented by a mixture of gases transforms into a "two-phase" or even "three-phase" state since, depending on the ambient conditions, clusters constituting a fine "phase" can be in both the liquid and solid states.

Water is among the most studied of chemicals, owing, in part, to its ubiquity and its necessity for all life. In addition to these "natural" reasons, water is an interesting compound because it has unique physical properties and is a model hydrogen-bonded liquid. Most of the available water interaction potentials are parametrized to reproduce the thermodynamic and structural properties of bulk water. The polarizable model allowed us to examine the changes in the dipole moment of the individual water molecules as a function of their environment. This can provide insight into many-body effects in water clusters at a molecular level. Dang and Chang (Dang & Chang, 1997) have developed a polarizable potential model for water that behaves reasonably well with changes in the environments (i.e.., cluster, liquid, and liquid/vapor). The simulation of water clusters was performed using a refined TIP4P interaction potential for water and the rigid four-center model of H_2O molecule (Jorgensen, 1981). The total interaction energy of the system can be written as

$$U_{\text{tot}} = U_{\text{pair}} + U_{\text{pol}} ,\qquad(3)$$

where the pairwise additive part of the potential is the sum of the Lennard-Jones and Coulomb interactions,

$$U_{\text{pair}} = \frac{1}{2}\sum_i\sum_j\left[4\varepsilon^{(\text{LJ})}\left\{\left(\frac{\sigma_{ij}^{(\text{LJ})}}{r_{ij}}\right)^{12} - \left(\frac{\sigma_{ij}^{(\text{LJ})}}{r_{ij}}\right)^{6}\right\} + \frac{q_iq_j}{r_{ij}}\right].\qquad(4)$$

Here, r_{ij} is the distance between site i and j, q is the charge, $\sigma^{(\text{LJ})}$ and $\varepsilon^{(\text{LJ})}$ are the Lennard-Jones parameters.

The nonadditive polarization energy is given by

$$U_{pol} = \frac{1}{2}\sum_i \mathbf{d}_i \cdot \mathbf{E}_i^0 ,\qquad(5)$$

where $\mathbf{E}_i^0$ is the electric field at site i produced by the fixed charges in the system

$$\mathbf{E}_i^0 = \sum_{j \neq i} \frac{q_j \mathbf{r}_{ij}}{r_{ij}^3} , \tag{6}$$

$\mathbf{d}_i$ is the induced dipole moment at atom site i, and is defined as

$$\mathbf{d}_i = \alpha_i^p \mathbf{E}_i , \tag{7}$$

where

$$\mathbf{E}_i = \mathbf{E}_i^0 + \sum_{j \neq i} \mathbf{T}_{ij} \cdot \mathbf{d}_j . \tag{8}$$

In the above, $\mathbf{E}_i$ is the total electric field at atom i, α_i^p is the atomic polarizability, and $\mathbf{T}_{ij}$ is the dipole tensor

$$\mathbf{T}_{ij} = \frac{1}{|r_{ij}|^3} \left(3\hat{\mathbf{r}}_{ij}\hat{\mathbf{r}}_{ij} - \mathbf{1} \right) . \tag{9}$$

In (9), $\hat{\mathbf{r}}_{ij}$ is the unit vector in the direction $\mathbf{r}_i - \mathbf{r}_j$, where $\mathbf{r}_i$ and $\mathbf{r}_j$ are the positions of the centers of mass of molecules i and j, and $\mathbf{1}$ is the 3 × 3 unit tensor.

The modification of interaction potential for water by Dang and Chang (Dang & Chang, 1997) concerned the variation of the parameters of the Lennard–Jones part of potential and localization of negative charge. As a result, the value of permanent dipole moment for water molecule was taken to be equal to its experimentally obtained value of 1.848 D. The geometry of this molecule corresponds to the experimentally obtained parameters of the molecule in the gas phase: r_{OH} = 0.09572 nm and angle HOH of 104.5° (Benedict et al., 1956). Fixed charges (q_H= 0.519 e, q_M= −1.038 e) are ascribed to H atoms and to point M lying on the bisectrix of angle HOH at a distance of 0.0215 nm from oxygen atom. The values of charges and the position of point M are selected so as to reproduce the experimentally obtained values of dipole and quadrupole moments (Xantheas, 1996; Feller & Dixon, 1996), as well as the ab initio calculated energy of dimer and the typical distances in the dimer (Smith & Dang, 1994). The stabilization of short-range order in water clusters is largely attained owing to the short-range Lennard-Jones potential with the center of interaction ascribed to the oxygen atom. Related to point M in addition to the electric charge is the polarizability which is required for the description of nonadditive polarization energy. The standard iterative procedure is used at every time step for calculating induced dipole moments (Dang & Chang, 1997). The accuracy of determination of $\mathbf{d}_i$ is given in the range of 10^{-5} –10^{-4} D.

The atom-atom impurity (carbon, oxygen, hydrogen, nitrogen)–water interactions were preassigned in terms of the sum of repulsion, dispersion, and Coulomb contributions,

$$\Phi(r_{ij}) = b_i b_j \exp[(c_i + c_j)r_{ij}] - a_i a_j r_{ij}^6 + \frac{q_i q_j}{r_{ij}} , \tag{10}$$

where the parameters a_i, b_i, and c_i of the potential describing these interactions were borrowed from Spackman (Spackman, 1986a, 1986b). Experimental polarizability values have been used (Lide, 1996).

The added linear CO_2, N_2O, CO, NO and C_2H_2 molecules were placed along the beams, connecting $(H_2O)_n$ cluster's center of the mass to those of these molecules. At first NO_2, O_3, CH_4 and C_2H_6 molecules were placed in the knots of imaginary BCC lattice piercing the cluster. In all cases the admixture molecules were situated outside the cluster.

The Gear method of fourth order was used for the integration of the motion equations of the molecules' centers of the mass (Gear, 1971). The analytical solution of motion equations for molecules' rotation was carried out with a help of the Rodrigues - Hamilton parameters (Petrov & Tikhonov, 2002). Scheme of the equations of motion integration at presence of rotation corresponded with the approach offered by Sonnenschein (Sonnenschein, 1985). The duration of calculation for each cluster lasted not less than $3 \cdot 10^6$ Δt, where time step was $\Delta t = 10^{-17}$ c.

The overall dipole moment of a cluster $\mathbf{d}_{cl}$ was calculated via the formula

$$\mathbf{d}_{cl}(t) = Z_+ \sum_{i=1}^{N_{tot1}} \mathbf{r}_i(t) + Z_- \sum_{j=1}^{N_{tot2}} \mathbf{r}_j(t) , \tag{11}$$

where $\mathbf{r}_i(t)$ is a vector denoting the position of atom i or point M at time moment t; Z_+ and Z_- are the electric charges located at positively and negatively sites; and N_{tot1} and N_{tot2} are the numbers of positively and negatively charged atoms in a cluster, respectively.

Static permittivity ε_0 was calculated from the fluctuations of overall dipole moment $\mathbf{d}_{cl}$ (Bresme, 2001) as follows:

$$\varepsilon_0 = 1 + \frac{4\pi}{3VkT} \Big[\langle \mathbf{d}_{cl}^2 \rangle - \langle \mathbf{d}_{cl} \rangle^2 \Big], \tag{12}$$

where V is the cluster volume and k is Boltzmann's constant.

Permittivity $\varepsilon(\omega)$ was represented as a function of frequency ω by a complex value $\varepsilon(\omega) = \varepsilon'(\omega) - i\varepsilon''(\omega)$, which was estimated through the following equation (Bresme, 2001; Neumann, 1985):

$$\frac{\varepsilon(\omega) - 1}{\varepsilon_0 - 1} = -\int_0^\infty \exp(-i\omega t) \frac{dF}{dt} dt = 1 - i\omega \int_0^\infty \exp(-i\omega t) F(t) dt , \tag{13}$$

where function $F(t)$ is the normalized autocorrelation function of the overall dipole moment of the cluster

$$F(t) = \frac{\langle \mathbf{d}_{cl}(t) \mathbf{d}_{cl}(0) \rangle}{\langle \mathbf{d}_{cl}^2 \rangle} . \tag{14}$$

Let us consider the scattering of nonpolarized light when the molecule path length l is much less than the light wavelength λ. The extinction (attenuation) coefficient ξ of an incident ray can be determined both by the Rayleigh formula (Landau & Lifshits, 1982)

$$\xi = \frac{2\omega^4}{3\pi c^4} \frac{(\sqrt{\varepsilon_0} - 1)^2}{N} , \tag{15}$$

and through the scattering coefficient μ by the expression ($\xi = \dfrac{16\pi}{3}\mu$) (Przhibel'sky, 1994) in the approximation of a scattering at an angle 90°. Here, N is the concentration of scattering centers, c is the light velocity, ε is the dielectric permittivity of the medium, and ω is the incident wave frequency.

Taking into consideration that $\xi = \alpha + \mu$, where α is the absorption coefficient, we obtain

$$N_{i,n} = \frac{2\omega^4}{3\pi c^4}\frac{(\sqrt{\varepsilon_0}-1)^2}{\alpha}(1-\frac{3}{16\pi})\cdot \tag{16}$$

Let us form system in such a way that the statistical weight of a cluster containing i admixture molecules and n water molecules can be expressed as follows:

$$W_{in} = \frac{N_{in}}{N_\Sigma}, \tag{17}$$

where N_{in} is the concentration of clusters with i admixture molecules and n water molecules, $N_\Sigma = \sum\limits_{i=1}^{n_i} N_i$, where n_i is the maximal value of i. Similar weights were used for $(H_2O)_n$ clusters constituting system. The further calculation of all the spectral characteristics was performed with consideration for the assumed statistical weights W_{in}. The average concentration of each type of cluster in the systems under consideration was 12–13 orders of magnitude lower than the Loschmidt number.

The absorption coefficient α of incident IR radiation can be expressed through the imaginary component of the frequency-dependent dielectric permittivity $\varepsilon(\omega)$ as follows (Neumann, 1986):

$$\alpha(\omega) = 2\frac{\omega}{c}\mathrm{Im}[\varepsilon(\omega)^{1/2}]. \tag{18}$$

In the case of depolarized light, the Raman spectrum $J(\omega)$ is determined as follows (Bosma et al., 1993):

$$J(\omega) = \frac{\omega}{(\omega_L - \omega)^4}\left(1 - e^{\hbar\omega/kT}\right) \times \mathrm{Re}\int_0^\infty \mathrm{d}t e^{i\omega t}\langle \Pi_{xz}(t)\Pi_{xz}(0)\rangle \tag{19}$$

where

$$\Pi(t) \equiv \sum_{j=1}^{N}\left[\alpha_j^p(t) - \langle\alpha_j^p\rangle\right], \tag{20}$$

$\hbar = h/2\pi$, h is the Planck constant, ω_L is the exciting laser frequency, Π_{xz} is the xz component of the $\Pi(t)$ value, the x axis is directed along the molecular dipole, and xy is the molecular plane.

The frequency dispersion of the dielectric permittivity determines the frequency dependence of dielectric losses $P(\omega)$ according to the equation (Levanuk & Sannikov, 1988)

$$P = \frac{\varepsilon'' < E^2 > \omega}{4\pi}, \qquad (21)$$

where $< E^2 >$ is the average squared intensity of an electrical field, and ω is the frequency of an emitted electromagnetic wave.

The rigid model of molecules used in this work does not permit consideration of intramolecular vibrations, which, as a rule, have frequencies $\omega > 1200$ cm^{-1}. In this work, we study the frequency range $0 \leq \omega \leq 1200$ cm^{-1}, which characterizes vibrational and rotational motions of molecules.

3. Water clusters and main greenhouse gases absorption

To determine the influence of absorbed polyatomic molecules on the greenhouse effect, we considered different types of ultradisperse systems: $(H_2O)_n$ (I), $(CO_2)_i(H_2O)_{10}$ (II), $(CH_4)_i(H_2O)_{10}$ (III), and $(N_2O)_i(H_2O)_{10}$ (IV), where $n = 10–20$ and $i = 1–10$. Investigation of clusterization of the GHG was executed in works (Galashev et al., 2006a, 2006b, 2007; Novruzov et al., 2006; Galasheva et al., 2007; Chukanov & Galashev, 2008; Galashev, 2011). Here we shall consider influence of capture of admixture molecules by water clusters on some spectral characteristics of cluster systems. In analyzing frequency-dependent characteristics we restrict ourselves to frequency range $0 \leq \omega \leq 1200$ cm^{-1} because no intramolecular vibrations are present in the model employed by us for systems I-IV. The structure of equimolecular heteroclusters is shown in Fig. 1, where configurations of $(CO_2)_{10}(H_2O)_{10}$ and $(CH_4)_{10}(H_2O)_{10}$ clusters are represented. One may observe that both clusters have a significantly irregular structure. Moreover, CO_2 molecules intermix with H_2O molecules and CH_4 molecules gather in one group forming heterocluster's surface. The correlation in the orientation of CO_2 and H_2O molecules can be observed, while CH_4 molecules are disoriented.

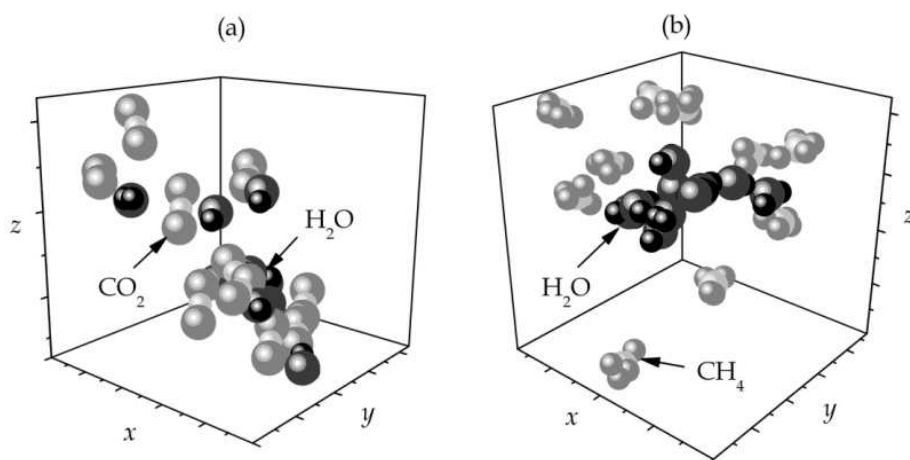Fig. 1. Configurations of clusters: (a) - $(CO_2)_{10}(H_2O)_{10}$, (b) - $(CH_4)_{10}(H_2O)_{10}$, corresponding to the moment of time 30 ps.

The greenhouse effect caused by atmospheric gases is in fact the absorption of the Earth's thermal radiation by them and a subsequent dissipation of the absorbed energy. The spectrum of Earth's thermal radiation, together with experimental IR radiation absorption

spectrum of liquid water (Goggin & Carr, 1986), is shown in Fig. 2(a). The spectrum for water overlaps practically all of the Earth's radiation frequency range and indicates the greatest significance of atmospheric moisture in greenhouse effect creation. The
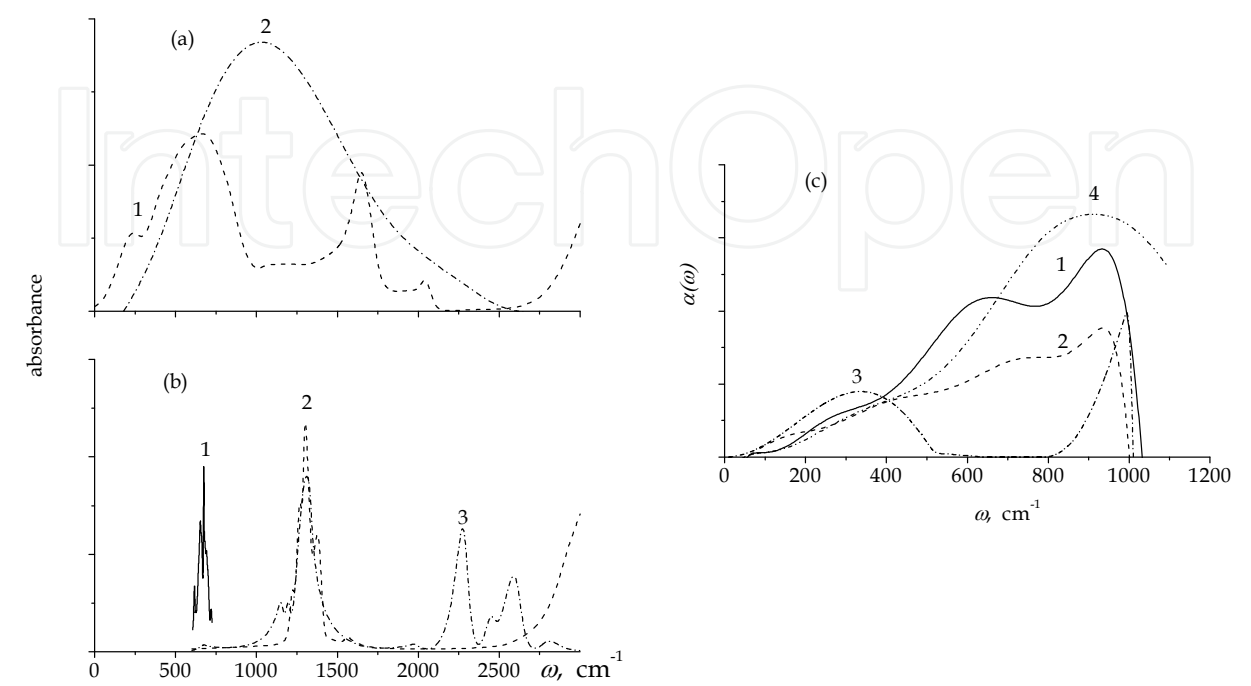
Fig. 2. IR absorption spectra, (a) *(1)* experimental spectrum for liquid water (Goggin & Carr, 1986), *(2)* spectrum of thermal radiation of the Earth at T = 280 K; (b) *(1)*, *(2)*, *(3)* experimental spectra for gaseous CO_2, CH_4, and N_2O (Kozintsev et al., 2003) correspondingly; (c) *(1)* system I, *(2)* II, *(3)* III, *(4)* IV.
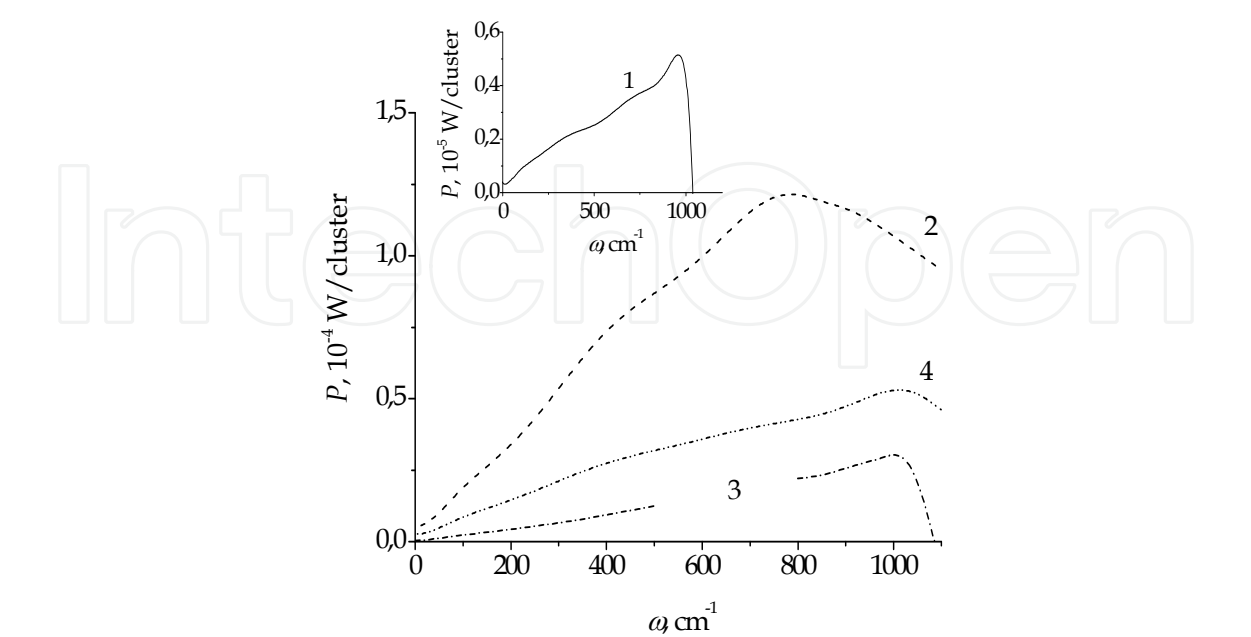
Fig. 3. The frequency dependence of dielectric loss for systems: *(1)* I (in the inset), *(2)* II, *(3)* III, *(4)* IV.

experimental IR spectra of gaseous CO_2, N_2O and CH_4 (Kozintsev et al., 2003) absorption are represented in Fig. 2(b). In the investigated frequency range the locations of the main spectrum peaks for gaseous N_2O and CH_4 coincide. These spectra represent a landmark for location of changes of relevant IR spectra peaks during transition from clusters of pure water to heteroclusters. IR spectra of systems I, II, III and IV presented in Fig. 2(c) are calculated by the method described in (Galashev et al., 2006b). The spectra for ultra-disperse systems of pure water and $CO_2)_i(H_2O)_{10}$ clusters system have two peaks, the main of which situates at ω = 974 (I) and 960 cm^{-1} (II), and the second peak at 661 cm^{-1} (I) and 724 cm^{-1} (II), it is less expressed. The IR spectra in the frequency range of $0 \leq \omega \leq 1200$ cm^{-1} related with aqueous systems containing N_2O and CH_4 molecules are characterized by one peak. These peaks are situated respectively at the 911 and 340 cm^{-1} frequency. In the observed frequency range the integral intensity of IR radiation absorption by systems II and III significantly decreases. On the contrary, for the system IV this value slightly increases in comparison with the corresponding characteristic of system I.

Let us consider energy exchange between photons representing falling electromagnetic wave and phonons – collective oscillations of molecules in clusters. The most probable events of this process are (Poulet & Mathieu, 1970):

1. the absorption of photon with frequency ω (or $\hbar\omega$ energy) with a birth of two phonons with the same ω_1 frequency extending in opposite directions under the law of energy conservation $\hbar\omega = 2\hbar\omega_1$ or $\omega = 2\omega_1$,
2. the absorption of photon with frequency ω causes appearance of two phonons with different frequencies ω_1 and ω_2, where $\omega = \omega_1 + \omega_2$,
3. the absorption of photon, the collapse of one phonon and the emergence of another with $\omega = \omega_1 - \omega_2$, $\omega_1 \neq \omega_2$.

The exchange of electromagnetic radiation energy with clusters is an essentially unharmonious process. Due to this the emerged phonon can be characterized not only by one frequency but by a number of frequencies from the appointed interval.

The most probable result of IR radiation interaction with clusters, as well as with crystals (Poulet & Mathieu, 1970), is the appearance of two phonons of the same frequency (event 1). We especially refer to this event at ω = 974 cm^{-1} frequency of the main IR spectrum peak of the system I. Then the frequency expected for appearing phonons is defined by ω_1 = 487 cm^{-1} value. The event 2 should be the second one according to the frequency occurrence where absorbed photon energy distributes among excited phonons in uneven portions. To this event we can attribute the emergence of the second IR spectrum peak in the system I at ω = 661 cm^{-1} frequency. The frequency $\omega_2 = \omega - \omega_1$ = 174 cm^{-1} can be thus derived. The third event of the system I, where the frequency of IR spectrum peak localization is defined by $\omega_1 - \omega_2$, is the least probable. In this case the location of expected peak is given by ω = 313 cm^{-1}. In the IR spectrum of the system I in the vicinity of this frequency (at 348 cm^{-1}) there is only one inflection point of dependence $\alpha(\omega)$. It is possible to estimate the influence of admixture molecules on clusters' phonons, and consequently, on corresponding IR spectra by inharmonic contributed by them. In the case of CO_2 molecules the interaction of clusters with IR radiation gives events 1 and 2, and the inharmoniousness is characterized by the quantities $\Delta\omega_1 = \omega_1(II) - \omega_1(I) = -7$ cm^{-1}, $\omega_2(II) - \omega_2(I) = 70$ cm^{-1} (II: ω_1 = 480 cm^{-1} and ω_2 = 280 cm^{-1}). The event 1 with phonon frequency ω_1 = 455.5 cm^{-1} takes place at interaction of IR radiation with $(N_2O)_i(H_2O)_{10}$ clusters, and the inharmoniousness is defined by the value $\Delta\omega_1(IV) = 31.5$ cm^{-1}. From the minimum unharmonious effect estimation it follows that for

$(CH_4)_i(H_2O)_{10}$ clusters the realization of event 3 with phonon frequencies $\omega_1 = 650$ cm^{-1} and $\omega_2 = 310$ cm^{-1} leading to a quantity of inharmoniousness $\Delta\omega_2(III) = 136$ cm^{-1}, is more probable. Thus, according to the quantity of contributed inharmoniousness (from greater to smaller) the admixture molecules locate as CH_4, CO_2, N_2O.

The frequency distribution of power dissipated by cluster systems under consideration is given in Fig. 3. One can see that the addition of CO_2, CH_4 and N_2O molecules to water clusters causes a significant increase in the rate of energy dissipation. The energy of absorbed IR radiation is dissipated most rapidly by system II with the maximum of dissipation at a frequency 800 cm^{-1}. The system IV has next rate of energy dissipation with a maximum of spectrum $P(\omega)$ at frequency 1036 cm^{-1}. The system of water clusters with absorbed CH_4 also strengthens IR radiation emission power. Water clusters exhibit the highest rate of dissipation of stored energy at frequency $\omega = 974$ cm^{-1}, and clusters which absorbed CH_4 molecules (system III) – at 1014 cm^{-1}.

4. Hydrocarbon molecules' absorption by ultra disperse water medium

We consider some types of ultra disperse systems: $(C_2H_2)_j(H_2O)_n$, $(C_2H_6)_j(H_2O)_n$, $(C_2H_2)_i(H_2O)_{20}$, $(C_2H_6)_i(H_2O)_{20}$, $j = 1, 2; 10 \leq n \leq 20, 1 \leq i \leq 6$. Configurations of (a) $(C_2H_2)_6(H_2O)_{20}$ and (b) $(C_2H_6)_6(H_2O)_{20}$ clusters corresponding to the moment of time 30 ps show the absence of stirring of H_2O molecules with C_2H_2 and C_2H_6 molecules even when the number of admixture molecules reaches six (Fig. 4). Acetylene molecules are attracted by water clusters. Finally, they get the orientation of a tangent to the $(H_2O)_{20}$ cluster surface. It is reached due to the attraction of C atoms to H atoms of water molecules oriented mainly outwards to the cluster. Thus, H atoms, which are on the ends of the C_2H_2 molecule, feel the repulsion from the surface of the water cluster. In this case, acetylene molecules act as proton acceptors (Allouch, 1999). Also, the bond energy with water clusters is estimated as – 13.8, –15.4 and –12.9 kJ/mol for systems $C_2H_6(H_2O)_n$, $(C_2H_6)_2(H_2O)_n$ and $(C_2H_6)_i(H_2O)_{20}$, respectively. These values are coordinated with the estimation of bond energy (–15.4 kJ/mol) for the acetylene acting as a proton acceptor to amorphous ice (Silva & Devlin, 1994).
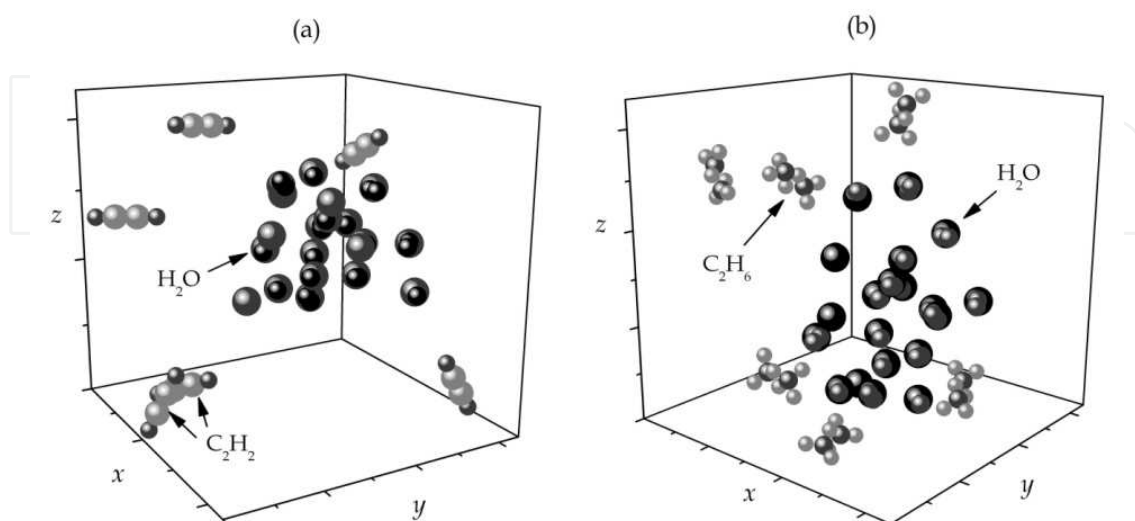

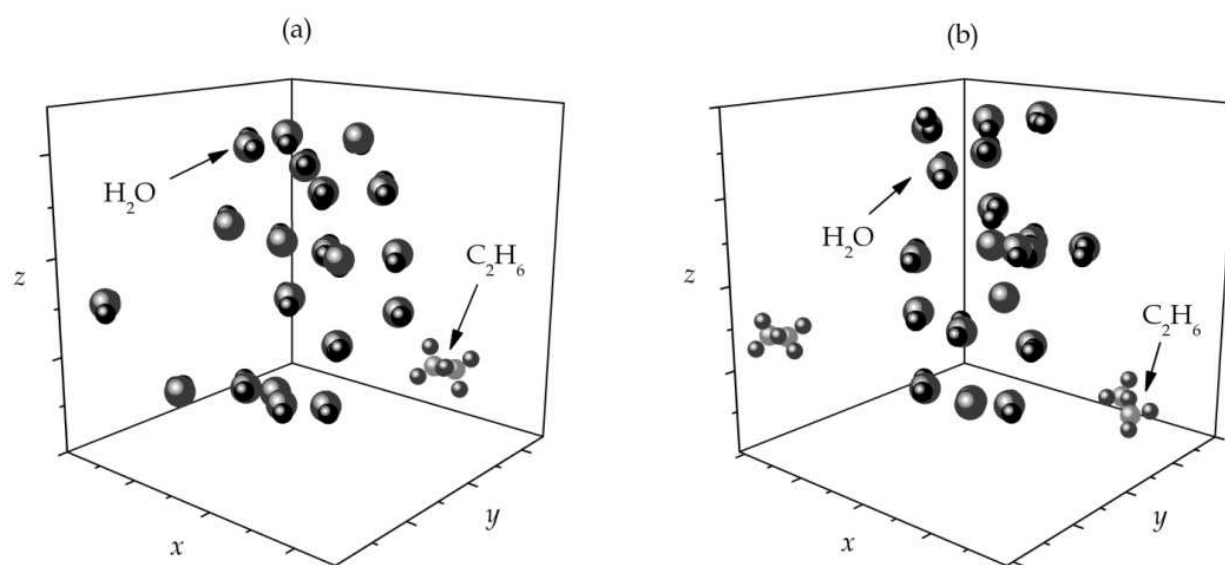Fig. 4. Configurations of (a) $(C_2H_2)_6(H_2O)_{20}$ and (b) $(C_2H_6)_6(H_2O)_{20}$ clusters, corresponding to the moment of time 30 ps.

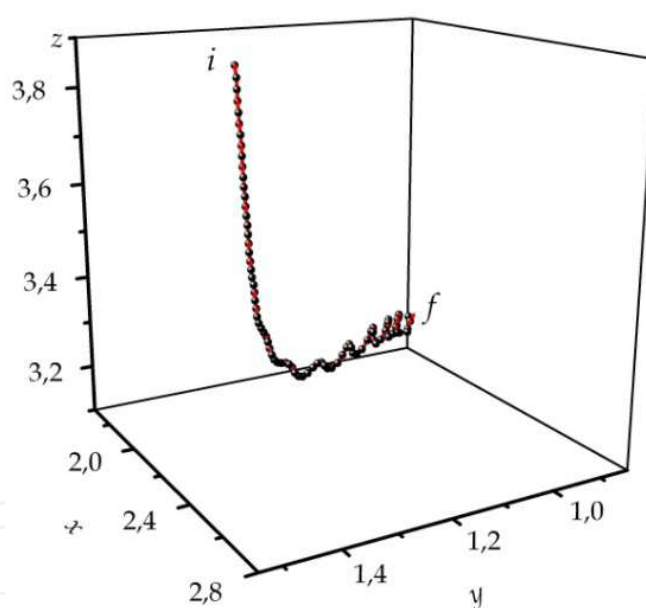Fig. 5. Configurations of the clusters corresponding to a time of 30 ps: (a) $C_2H_6 (H_2O)_{20}$ and (b) $(C_2H_6)_2(H_2O)_{20}$ clusters.

Fig. 6. Trajectory of motion for the center of mass of the C_2H_2 molecule within 30 ps: i and f are the beginning and the end of the trajectory, respectively. The coordinates are given in units $\sigma_w = 0.3234$ nm.

The bond energy for acetylene–water dimer is determined at –(5.0–7.9) kJ/mol (acetylene–proton acceptor) and –(8.7–13.3) kJ/mol (acetylene–proton donor) (Frish et al., 1983). Interaction of ethane molecules with water clusters is characterised by higher values of bond energy. These values for systems of $C_2H_6(H_2O)_n$, $(C_2H_6)_2(H_2O)_n$ and $(C_2H_6)_i(H_2O)_{20}$ are –11.7, –11.7 and –6.7 kJ/mol, respectively. If, in general, for the first two systems, the ethane acts as a proton acceptor, then for the last system, it acts as a proton donor (oxygen–hydrogen of

ethane pairs gives the lowest energy in the ethane–water interaction). Thus, with the growth of ethane concentration and the amplification of interaction between C_2H_6 molecules, the switching of the bond type from the proton acceptor to the proton donor is observed. Bond energy in a complex amorphous ice–ethylene (proton acceptor) is estimated as –15.8 kJ/mol (Silva & Devlin, 1994). At atmospheric pressure, the ethylene has the higher solubility in water than ethane. The C_2H_6 molecules are not rejected by water cluster but also do not approach it too close being symmetrically on opposite sides of the cluster.

Theoretical determination of the ground-state geometry of water clusters is a difficult task. As the number of local minima grows exponentially with the number of atoms, finding the global minimum is a real challenge. Exact definition of the cluster configurations with the minimal energy is complicated due to energies, corresponding to the different equilibrium configurations, that are close enough. These configurations frequently differ only in the way of arrangement of atoms of hydrogen in the system of bonds. Already for polytetrahedral clusters from eight molecules, the number of isomers formed due to the hydrogen disorder makes 450, and it is already more than 40,000 of such isomers for similar clusters from 14 molecules (Kirov, 1993). Another difficulty is that the use of various models of water results in clusters with the minimal energy, having various forms. In addition, their structures differ by symmetry (Sremaniak et al., 1996). Even with the use of the same model of water, different forms of the $(H_2O)_{20}$ clusters with the minimal energy were received. With the help *ab initio* calculations, using TIP4P potential, Tsai and Jordan (Tsai & Jordan, 1993) have defined such cluster in the form of the fused cube, and by a method of molecular dynamics with the same potential Wales and Ohmine (Wales & Ohmine, 1993) have found an even lower energy structure for $(H_2O)_{20}$, which consists of three pentagonal prisms sharing three faces. Extensive *ab initio* calculations have been performed for several possible structures of water clusters $(H_2O)_n$, n=8–20 (Stern & Berne, 2001). It is found that the most stable geometries arise from a fusion of tetrameric or pentameric rings. As a result, $(H_2O)_n$, $n = 8$, 12, 16 and 20, are found to be cuboids, while $(H_2O)_{10}$ and $(H_2O)_{15}$ are fused pentameric structures. It is necessary to notice that the adding polarisability in an explicit manner has the effect favouring a reduction in strain energy at the expense of hydrogen bonding (Sremaniak et al., 1996). Many-body intermolecular interaction expansions provide a promising avenue for the efficient quantum mechanical treatment of molecular clusters and condensed-phase systems, but the computationally expensive three-body and higher terms are often non-trivial (Maheshwary et al., 2001).

The neighbourhood already with one ethane molecule changes the structure of water cluster. The C_2H_6 molecules are not detached by the water core of a cluster; however, at the same time, they do not approach the core too closely (Fig. 5). In the case of both clusters, every C_2H_6 molecule is adjacent to three water molecules. Also, every C_2H_6 molecule is oriented arbitrarily to the water core of a cluster, i.e. its C–C axis is directed neither at the centre of a cluster mass nor tangentially to the core "surface". The presence of a second C_2H_6 molecule changes the shape of the water skeleton of a cluster. This is due to the fact that every ethane molecule adjusts the nearest water molecules of a cluster to its conformation. The C_2H_6 molecules are quite remote from water molecules comparing to the distance between the adjacent H_2O molecules. In general, the surface of the $C_2H_6(H_2O)_{20}$ cluster turned out to be looser than the surface of the $(C_2H_6)_2(H_2O)_{20}$ cluster. The structures shown in Fig. 4 and 5 correspond to the energy close to the minimal one for these clusters under considered conditions.

The motion of the center of mass of one of the C_2H_2 molecules during the formation of the cluster $(C_2H_2)_2(H_2O)_{20}$ is reflected by the trajectory depicted in Fig. 6. The trajectory was followed over the time span of 30 ps. The initial and final positions of the center of mass of the molecule are denoted by the symbols i and f, respectively. It is seen that the C_2H_2 molecule first moves strictly rectilinearly toward the cluster. Covering a certain distance, the molecule turns toward the tangent to the cluster surface and follows in this direction, experiencing small-scale oscillation.

The frequency dependence of $\alpha(\omega)$ IR radiation absorption coefficient of investigated systems is shown in Fig. 7. The $\alpha(\omega)$ coefficient for disperse systems containing C_2H_2 molecules is higher than that for the disperse system of pure water (Fig. 7(a)). The intensity of the spectrum is increased with the growth of C_2H_2 molecules' number in the water system. The principal maximum of the $\alpha(\omega)$ distribution for the system of pure disperse water falls in the frequency of 780 cm^{-1}, and that for the similar water system with one and two acetylene molecules in each cluster is at 970 cm^{-1}. After absorption from one up to six acetylene molecules by the monodisperse water system, the $\alpha(\omega)$ spectrum becomes strongly oscillating with the principal maximum at $\omega = 920$ cm^{-1}. The $\alpha_w(\omega)$ spectrum of bulk liquid water (Goggin & Carr, 1986) has two maxima at frequencies of $\omega = 200$ and 690 cm^{-1}. The higher integrated intensity of IR radiation absorption for bulk water is caused by its density, which is higher, on average, than the density of water clusters by a factor of 1.4. However, in the presence of hydrocarbon molecules in these clusters, the density is not a determining factor in the absorption of IR radiation. The expansion of the system owing to the attachment of hydrocarbon molecules results in an increase in the number of vibration modes including the $0 \leq \omega \leq 1000$ cm^{-1} frequency range of the $\alpha(\omega)$ spectrum. The orientation of acetylene molecules on a tangent to the water cluster gives a stable amplification of the integrated intensity of the $\alpha(\omega)$ spectrum with the growth of acetylene concentration. This is promoted by the repulsion of the positive charges of C_2H_2 molecules. The bending band of the $\alpha(\omega)$ spectrum of gaseous acetylene is located at a frequency of $\omega = 730$ cm^{-1} (Kozintsev et
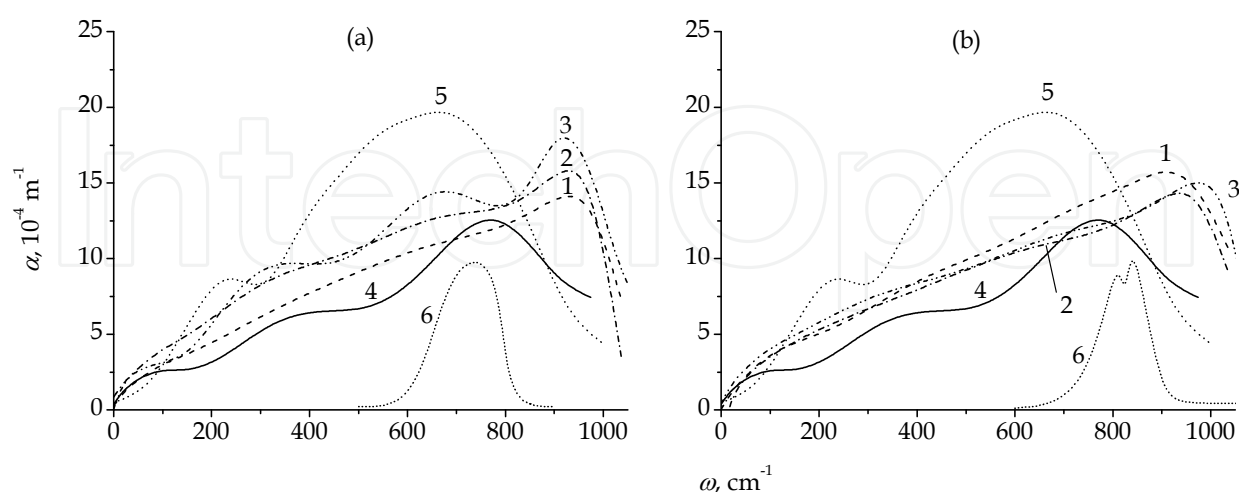

Fig. 7. Absorption coefficient of IR radiation for cluster systems: (a) 1, $C_2H_2(H_2O)_n$; 2, $(C_2H_2)_2(H_2O)_n$; 3, $(C_2H_2)_i(H_2O)_{20}$. (b) 1, $C_2H_6(H_2O)_n$; 2, $(C_2H_6)_2(H_2O)_n$; 3, $(C_2H_6)_i(H_2O)_{20}$; 4, $(H_2O)_n$; 5, $\alpha_w(\omega)$ function of bulk water, experiment (Goggin & Carr, 1986) and 6, experimental spectrum for gaseous hydrocarbon: (a) C_2H_2 and (b) C_2H_6 (Kozintsev et al., 2003).

al., 2003). Thus, the attachment of acetylene molecules by water clusters strengthens the integrated I_{tot} absorption intensity.

Ethane molecules have the more chaotic orientation. This results in a more random change of the vibrations' intensity with the growth of the number of C_2H_6 molecules in clusters. As a consequence, the behaviour of the IR absorption spectrum for these systems is less stable when the number of C_2H_6 molecules changes. After absorption of one ethane molecule, the absorption of external IR radiation in the investigated frequency range by ultradispersed water systems is also amplified (Fig. 7(b)) and the form of the curve becomes smoother. However, the following addition of C_2H_6 molecules results in some decrease of the IR radiation absorption, at least at frequencies of $\omega > 310$ cm^{-1}. The values of the α coefficient for the systems consisting of heteroclusters are higher than that for a cluster system of pure water almost in all frequency ranges (except for the area of $690 \leq \omega \leq 800$ cm^{-1}). The principal maximum of the $\alpha(\omega)$ frequency spectrum appears at $\omega = 910$ cm^{-1} (C_2H_6 $(H_2O)_n$ system) and $\omega = 973$ cm^{-1} (($C_2H_6)_2(H_2O)_n$ and $(C_2H_6)_i(H_2O)_{20}$ systems). The part of the $\alpha(\omega)$ spectrum determined by the bending vibrations of gaseous ethane molecules has the doubled maximum in the $810 \leq \omega \leq 840$ cm^{-1} frequency range (Kozintsev et al., 2003).

Water clusters including clusters absorbing acetylene or ethane molecules are capable of re-emitting the falling IR radiation. Calculations show that the disperse system consisting of pure water clusters has low values of P radiation power, in comparison with the system enriched with acetylene (Fig. 8(a)). For the disperse system formed by pure water, two characteristic frequencies of IR radiation are observed: $\omega_1 = 657$ cm^{-1} and $\omega_2 = 973$ cm^{-1}. The maximal value of emitted radiation power corresponds to a frequency of 970 cm^{-1} when only one C_2H_2 molecule is present in the clusters, and to a frequency of 910 cm^{-1} at the presence of two acetylene molecules in every cluster of the system. After adsorption of the second C_2H_2 molecule by clusters, the radiation power of disperse systems is increased. Moreover, the absorption of ethane molecules by water clusters causes the essential decrease of clusters' P radiation power (Fig. 8(a), insert). Arrangement of C_2H_2 molecules on a tangent to a surface of water clusters makes their structure more dense (Novruzov et al., 2008a). Due to

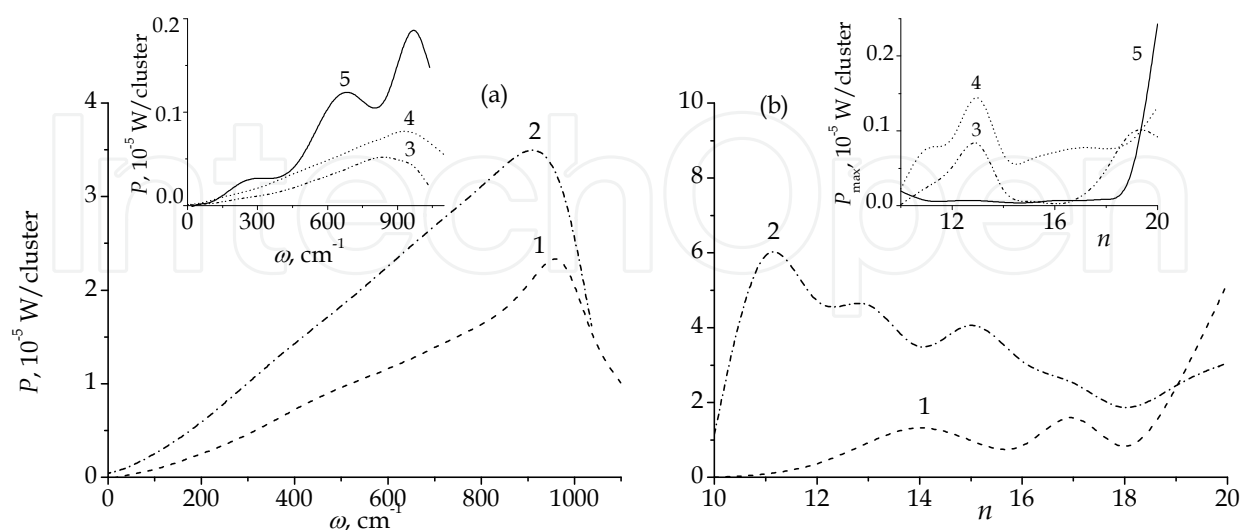

Fig. 8. Frequency dependence of (a) $P(\omega)$ IR radiation power and (b) maximum P quantity on n number of water molecules in clusters: 1, $C_2H_2(H_2O)_n$; 2, $(C_2H_2)_2(H_2O)_n$; 3, $C_2H_6(H_2O)_n$; 4, $(C_2H_6)_2(H_2O)_n$; 5, $(H_2O)_n$.

C atoms, the acetylene molecule is attached to the cluster. Due to H atoms, the molecule keeps a tangent direction to the water cluster and makes it denser. As a rule, $\bar{n}_b$, an average number of hydrogen bonds per molecule, decreases, and $\bar{L}_b$, the H-bond length, increases during the addition of both acetylene and ethane molecules to water clusters (Novruzov et al., 2008a, 2008b). When the number of admixture molecules $i < 5$, the value of $\bar{n}_b$ for water clusters with C_2H_2 molecules is higher and $\bar{L}_b$ is lower than those for clusters with C_2H_6 molecules. The volume of water clusters with C_2H_2 molecules appears to be 5–10% less than the volume of similar clusters with C_2H_6 molecules. As a result, the D_w self-diffusion coefficient of water molecules in $(C_2H_2)_i(H_2O)_n$ clusters is on average 20–30% lower than that in $(C_2H_6)_i(H_2O)_n$ clusters. The D_a self-diffusion coefficient of C_2H_2 molecules is higher than the D_a value of C_2H_6 molecules by no more than 1%. The decrease of the D_w value causes the amplification of collective vibrations, which, in turn, causes an appreciable amplification of dissipation of absorbed energy. An average $\bar{d}_{cl}$ dipole moment of $(C_2H_2)_i(H_2O)_n$ clusters exceeds the appropriate $\bar{d}_{cl}$ value of $(C_2H_6)_i(H_2O)_n$ clusters on an average by 5%. The ε'' imaginary part of dielectric permittivity of $(C_2H_2)_i(H_2O)_n$ clusters can increase by an order in comparison with the ε'' value of pure water clusters. This causes a sharp amplification of emitted radiation power for the system formed from these clusters. For $(C_2H_6)_i(H_2O)_n$ clusters, the opposite picture is observed, i.e. the ε'' value significantly reduces (up to five times), which causes an appreciable easing of the power of emitted IR radiation by an appropriate cluster system. The $P(\omega)$ spectra for the systems consisting of heteroclusters become smoother than those for the clusters system of pure water. The doubling of C_2H_6 molecules' number in ultra disperse system results in some amplification of radiation power. The principal maxima of the $P(\omega)$ spectra for the systems containing one and two ethane molecules in clusters are located at ω = 847 and 910 cm^{-1}, respectively.

The behaviour of the P_{max} maximal value of clusters in dependence on a number of water molecules containing in clusters is shown in Fig. 8(b). Pure water clusters are characterised by an extremely low rate of energy dissipation up to the size $n = 18$ (an insert in Figure 8(b)). For $(H_2O)_n$ clusters with $n > 18$, the radiation power is sharply increased, but still remains low enough in comparison with the similar characteristic of clusters containing C_2H_2 molecules. The maximal values of the radiation power of water clusters adding one C_2H_2 molecule up to the size $n = 18$ are considerably lower than the P_{max} quantity of $(C_2H_2)_2(H_2O)_n$ clusters. Almost everywhere, the P_{max} values for clusters of the system where each aggregate contains two ethane molecules exceed the appropriate characteristics of aggregates of the system with one C_2H_6 molecule. At the same time, clusters containing ethane molecules, as a rule, have the higher P_{max} values than pure water clusters. Water clusters with $n = 10$, 16 and 20 are an exception here.

5. Characteristics of water clusters in the presence of nitrogen dioxide

For a system consisting of $(NO_2)_i(H_2O)_{50}$, heteroclusters, the $\alpha(\omega)$ spectrum becomes more rough than for clusters system of pure water (Fig. 9(a)). The integral intensity ratio between the absorption spectra for the system of pure water clusters (I_1) and the system of water heteroclusters containing i number of NO_2 molecules (I_2) is $I_1 : I_2 = 1 : 0.95$. For the system of pure water clusters, the spectrum of the absorption coefficient demonstrates one maximum at 838 cm^{-1} (curve 1), whose localization disagrees with that of the main peak in the experimental absorption spectrum of bulk water, ω = 690 cm^{-1} (curve 3). The IR absorption spectrum of liquid water also comprises a slightly pronounced peak in the vicinity of $\omega \approx$

200 cm^{-1} (Goggin & Carr, 1986). The discrepancy in the positions of the main peaks may be related to the fact that the collective vibrations of the dipole moments of molecules in the clusters as nanosized objects may be characterized by frequencies different from the corresponding characteristics of liquid water. In the $\alpha(\omega)$ spectrum of heteroclusters (curve 2), four peaks are distinguished at ω = 88, 338, 713, and 901 cm^{-1} (the main maximum). In the examined frequency range, a local maximum is present at ω = 780 cm^{-1} in the experimental absorption spectrum of gaseous nitrogen(IV) dioxide (curve 4). The high-frequency maxima are observed in the absorption spectrum of NO$_2$ at ≈1300, 1650, and 1900 cm^{-1} (Kozintsev et al., 2003).

The IR absorption spectra obtained for single clusters of the $(NO_2)_i(H_2O)_{50}$ system, $0 \leq i \leq 6$ are illustrated in Fig. 9(b). The maximum integral intensity is inherent in the clusters containing 3 nitrogen (IV) dioxide molecules. On average, the spectra comprise three to four peaks, with the most intense peak being most often located in the frequency range $800 \leq \omega \leq 1000$ cm^{-1}. The exception is the $\alpha(\omega)$ spectrum of the pure water cluster whose main maximum is observed at 680 cm^{-1}. As awhole, the spectral intensities are comparable; the ratio between the maximum I_{max} and the minimum integral intensity I_{min} is 1.12. Even the addition of one impurity molecule can markedly change the pattern of an absorption spectrum.

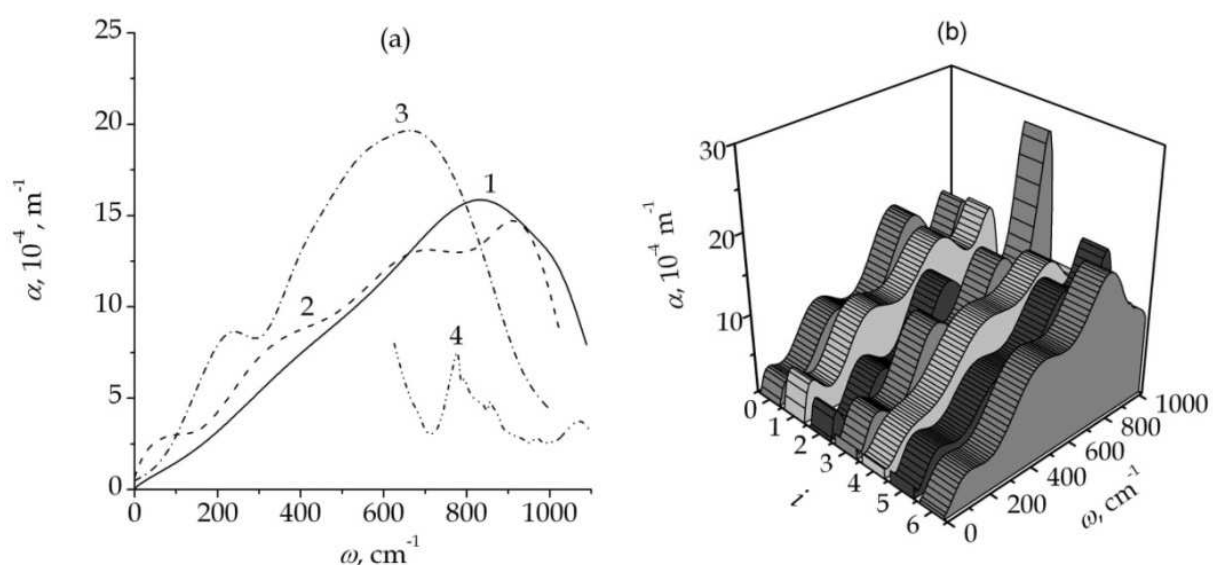Fig. 9. (a) Frequency dependences of the IR absorption coefficients for different systems: (1) $(H_2O)_n$ at $10 \leq n \leq 50$, (2) $(NO_2)_i(H_2O)_{50}$ at $1 \leq i \leq 6$, (3) the experimental spectrum of bulk liquid water (Goggin & Carr, 1986), and (4) experimental spectrum of gaseous NO$_2$ (Kozintsev et al., 2003); (b) IR absorption coefficients for $(NO_2)_i(H_2O)_{50}$ clusters at $0 \leq i \leq 6$.

The scattering of electromagnetic waves by molecules of a substance takes place due to the fact that the electric field of an electromagnetic wave induces a dipole moment in a molecule and this moment vibrates at the frequency of the field. At weak electric fields, the induced dipole moment is proportional to the field strength, with the molecule polarizability playing the role of the proportionality coefficient. According to the classical physics, the mechanism of the scattering of incident electromagnetic waves by molecules lies in the fact that molecules emit secondary electromagnetic waves with the frequencies of the primary incident waves. However, because the polarizability of a molecule depends on the interatomic distances in it and varies with time during its vibration, the spectrum of a

scattered light is transformed. In addition to the lines corresponding to the frequencies of the incident light, lines corresponding to the combinations (sums and differences) of these frequencies and normal vibration frequencies arise in the spectra (Günzler, H. & Gremlich, 2002).

A Raman spectrum consists of a most intense line (the exciting line) with the frequency equal to that of the incident radiation and less intense lines on each side of the former. The lines on the side of higher frequencies (the anti-Stokes lines) are noticeably less intense than those on the side of lower frequencies (the Stokes lines) (Wilson et al., 1980). Figure 10(a) depicts the anti-Stokes regions of the Raman spectra for $(H_2O)_{50}$ cluster (curve *1*) and $(NO_2)_i(H_2O)_{50}$ system (curve *2*), which comprise peaks with close positions but different intensities. The shown pattern of the spectra reflects the shifts relative to the exciting frequency $\omega_L = 19436.3$ cm^{-1} (the green line of the argon laser, $\lambda = 514.5$ nm).
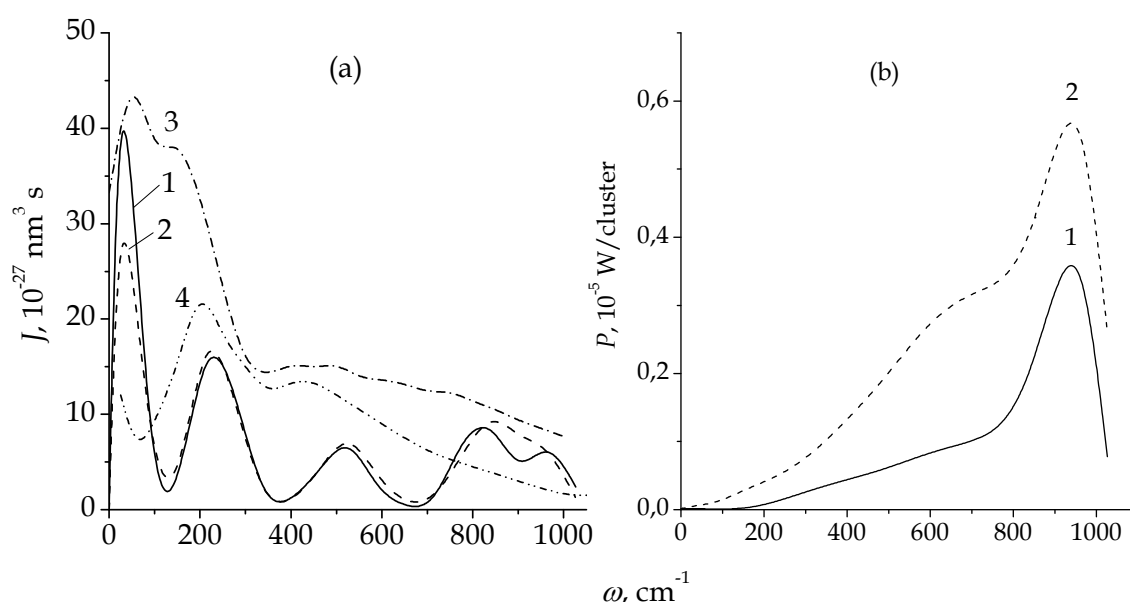

Fig. 10. (a) Raman spectra for (1) $(H_2O)_{50}$ cluster and (2) $(NO_2)_i(H_2O)_{50}$ system with $1 \leq i \leq 6$, (3) experimental spectrum of bulk water (Murphy, 1977), (4) spectrum calculated for a $(H_2O)_{50}$ cluster by molecular dynamic method using SPC/E three-site rigid model of water molecule (Bosma et al., 1993); (b) IR emission spectra for different systems: (1) $(H_2O)_n$ at $10 \leq n \leq 50$ and (2) $(NO_2)_i(H_2O)_{50}$ at $1 \leq i \leq 6$.

A distinct line with the frequency 30 cm^{-1} is the first reflection of the exciting frequency. A fainter line ($\omega = 220$ cm^{-1}) located in the immediate proximity to the exciting line is related to a change in the state of the rotational energy within the limits of the same vibrational state (Wilson et al., 1980). In the vibrational IR and Raman spectra of liquid water, the low-frequency region ($30 \leq \omega \leq 300$ cm^{-1}) resulting from the displacements of oxygen atoms (intermolecular motions) and the high-frequency region (higher than 3000 cm^{-1}) resulting from the modes of hydrogen atoms (intramolecular stretching vibrations of O–H bonds) are distinguished between (Agmon, 1996). The short-range order with the tetrahedral symmetry is created by complexes composed of five water molecules. Four normal modes are distinguished between in the tetrahedral symmetry, i.e., the breathing mode (ω_1) which describes completely nondegenerate symmetric stretching; the twice degenerate torsional mode (ω_2); two three-times degenerate modes, i.e., asymmetric stretching (ω_3) and bending

(ω_4). In the Raman spectrum of water, all four modes must be active, with the following values attributed to them: $\omega_4 = 50$ cm^{-1}, $\omega_2 = 70$ cm^{-1}, $\omega_1 = 150$ cm^{-1}, and $\omega_3 = 180$ cm^{-1} (Agmon, 1996). The first peak ($\omega = 30$ cm^{-1}) in the Raman spectrum obtained for water clusters may be interpreted as the confluence of modes ω_2 and ω_4, whereas the second peak (at 220 cm^{-1}) may be considered as the combination of modes ω_1 and ω_3. Hence, the even (ω_2 and ω_4) and odd (ω_1 and ω_3) tetrahedral modes exhibit the red and blue shifts, respectively.

Proton mobility in water is characterized by jump time τ which, at room temperature, is ≈ 1.5 ps (Agmon, 1996). Time τ is determined from the data on the narrowing of NMR signals (Halle & Karlstrom, 1983). This time reflects the abnormal mobility of protons in water upon a jump 0.25–0.26 nm long. The time τ of the fast reorientation in water may be related to the intensity of the Raman peak assigned to the asymmetric stretching of the tetrahedron, i.e. the ω_3 frequency. For a system of clusters, this peak corresponds to a frequency of 220 cm^{-1}. Under the four-coordinated water approximation, hydrogen bonds are reoriented at a constant rate of $I_{\omega 3}/\tau$. It can be assumed that this rate is independent of temperature and, at equilibrium, we have $\tau \sim I_{\omega 3}$. For the examined clusters, the half-width of the Raman peak at 220 cm^{-1} is nearly 130 cm^{-1} and slightly varies with changes in their composition. A proton mobility time of ≈ 0.26 ps corresponds to this half-width. It is seen that the evaluation time of the reorientation of hydrogen bonds in clusters containing 50 water molecules is decreased by a factor of five to six as compared to τ of liquid water. This time, which is predetermined by the number of water molecules in a cluster and temperature, slightly varies as the cluster uptakes NO$_2$ molecules. Note that the estimation of τ is of an approximate character, because the peak at 220 cm^{-1} is predetermined by both the mode and the symmetric location of the tetrahedron of water molecules with frequency ω_1. Therefore, the real time τ of the clusters must be longer.

The lines located farther from the exciting line, $\omega = 526$ and 838 cm^{-1}, are attributed to simultaneous changes in the vibrational and rotational energy states. The Raman spectra comprise overtones which, ignoring anharmonicity, represent the combinations of the exciting frequency and frequencies divisible by the frequency (~ 200 cm^{-1}) of vibrational–rotational transitions. In the Raman spectrum of (H$_2$O)$_{50}$ clusters (curve 1), the peak at 838 cm^{-1} can be considered to be an overtone of the peak at 220 cm^{-1}. The experimental spectrum of bulk water (curve 3) demonstrates three peaks at ω=53, 143 and 447 cm^{-1} (Murphy, 1977). According to our calculations, the first of these peaks is somewhat shifted to the left and is located at $\omega = 30$ cm^{-1}. Curve 4 corresponds to the Raman spectrum of a pure water cluster consisting of 50 molecules and obtained in terms of the molecular dynamic model using the SPC/E rigid three-site polarizable model of a water molecule (Bosma et al., 1993). In this case, two peaks are observed, i.e., one at $\omega = 200$ cm^{-1} that is in good agreement with our calculations, and another at 450 cm^{-1}. The latter peak appears to be somewhat shifted to the red relative to the position of the corresponding peak in the Raman spectrum that we calculated for the cluster, for which $\omega = 526$ cm^{-1}. At frequencies higher than 550 cm^{-1}, the spectrum of the SPC/E cluster is a long damped tail, while, in the $J(\omega)$ spectrum of a modified TIP4P model, vibrations with maxima at 838 and 963 cm^{-1} are observed.

The power of scattering the energy accumulated in the systems of clusters is presented in Fig. 10(b). The rate of the energy scattering for heteroclusters containing nitrogen(IV) oxide is 2.3-fold higher than that for pure water clusters, with the most intense peaks being located at a frequency of 963 cm^{-1} in both cases. The $P(\omega)$ spectra are, in both cases, unimodal. However, in the $P(\omega)$ spectrum of the heteroclusters, a shoulder arises in the vicinity of $\omega \approx 700$ cm^{-1}.

6. Spectral characteristics of the ozone-water cluster system

Let us consider the dielectric properties for two cluster systems: $(H_2O)_n$, $10 \leq n \leq 50$ (I') and $(O_3)_i(H_2O)_{25}$, $0 \leq i \leq 6$ (II'). The configuration of an $(O_3)_6(H_2O)_{25}$ cluster corresponding to the time moment of 30 ps is shown in Fig. 11. It can be seen that the cluster central part (skeleton) consisting of water molecules has an elongated form. Ozone molecules evenly surround the skeleton formed by water molecules and do not strive to get inside it. The orientation of ozone molecules is caused by the character of their contact with the water skeleton. An ozone molecule is bonded with one or, more rarely, two water molecules. As a rule, the side atoms of O_3 molecules are located more closely to the hydrogen atoms of H_2O molecules. A nonlinear O_3 molecule had one positive (q_{cen}) and two negative (q_{side}) charges placed at the localization points of the central and side atoms, respectively. Since the hydrogen atoms are mainly oriented outward from the water skeleton, the central atom of three of six O_3 molecules is oriented outwards. The molecular planes of two O_3 molecules are positioned tangentially to the skeleton, and the central atom of one O_3 molecule is closer to the water skeleton than its side atoms.
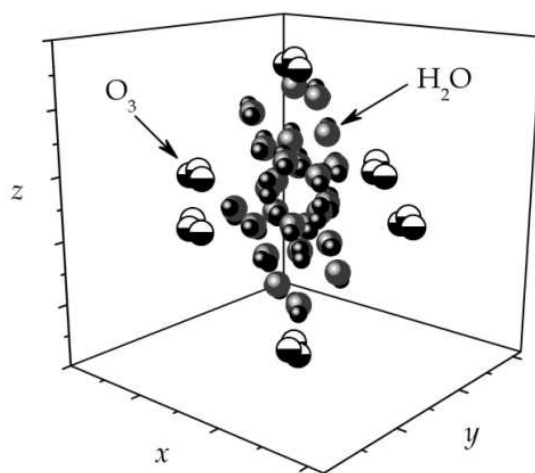

Fig. 11. Configuration of the $(O_3)_6(H_2O)_{25}$ cluster at a time moment of 30 ps.

The IR absorption spectrum $\alpha(\omega)$ of the disperse water system is appreciably changed after ozone has been absorbed (Fig. 12(a)). The main peak in the $\alpha(\omega)$ spectrum of the pure water system at a frequency of 843 cm^{-1} is transformed into two peaks corresponding to the frequencies of 690 and 970 cm^{-1}. The location of the first of these peaks coincides with that of the main peak in the IR absorption spectrum of bulk water (Goggin & Carr, 1986), and the second one is positioned close to the peak typical of the atmospheric ozone spectrum $\alpha(\omega)$ obtained by a satellite at a height of 83 km (Fichet et al., 1992). The absorption of ozone leads to a 14.1% decrease in the integral intensity of the IR absorption spectrum of the disperse water system.

The IR absorption spectra of individual $(O_3)_i(H_2O)_{25}$ clusters are illustrated in Fig. 12(b). It can be seen that their shapes and the intensities of peaks are substantially changed with addition of new ozone molecules to a water cluster. The $\alpha(\omega)$ spectra of the clusters forming system II' have two to four peaks. The integral intensity I_{tot} of the $\alpha(\omega)$ spectrum is minimal for the $(O_3)_6(H_2O)_{25}$ cluster and maximal for the $(O_3)_4(H_2O)_{25}$ aggregate. The value of I_{tot} of the clusters of system II' changes within 25.0%, and that of the water clusters, which have

captured from two to five ozone molecules, becomes ~10.8% higher on average in comparison with I_{tot} of the $(H_2O)_{25}$ cluster.
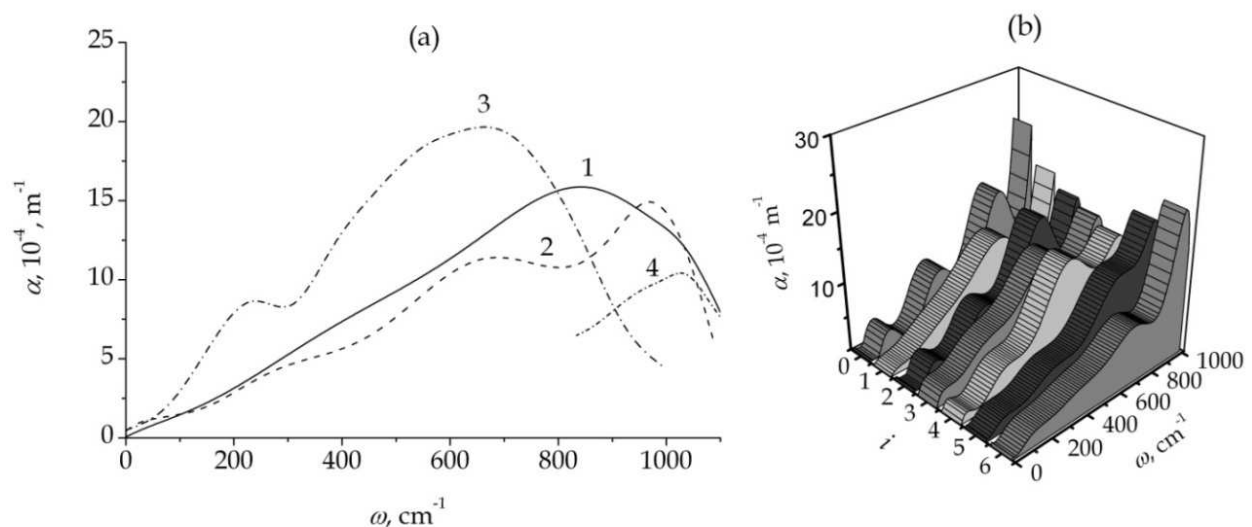

Fig. 12. (a) IR absorption spectra of (1) $(H_2O)_n$, $10 \leq n \leq 50$ and (2) $(O_3)_i(H_2O)_{25}$, $1 \leq i \leq 6$ systems; (3) the experimental $\alpha(\omega)$ function of bulk liquid water (Goggin & Carr, 1986); and (4) experimental spectrum of gaseous O_3 (Fichet et al., 1992); (b) IR absorption spectra of $(O_3)_i(H_2O)_{25}$ clusters, $0 \leq i \leq 6$.

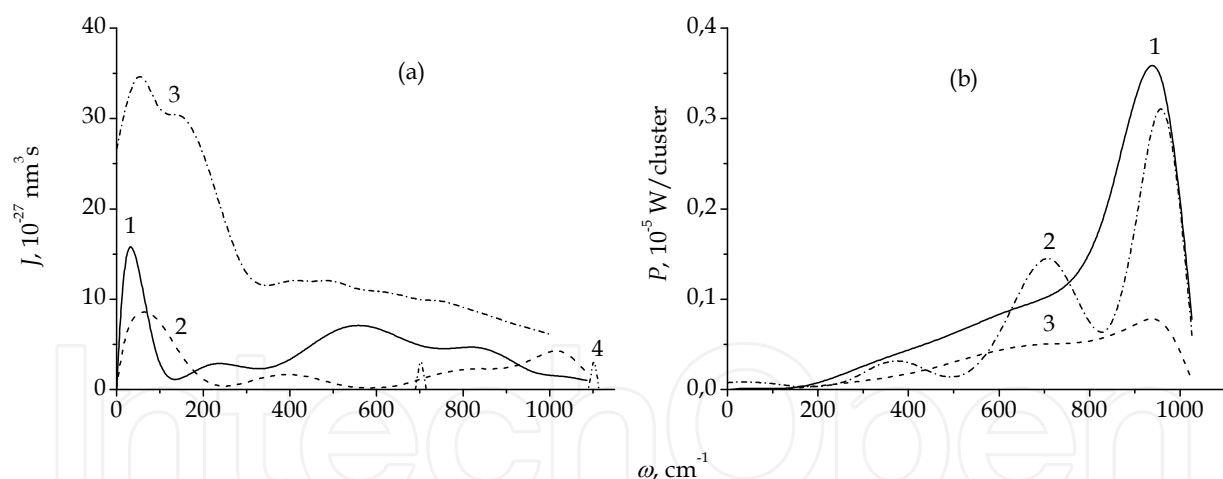Fig. 13. (a) Raman spectra of (1) $(H_2O)_n$, $10 \leq n \leq 50$ and (2) $(O_3)_i(H_2O)_{25}$, $1 \leq i \leq 6$ systems; (3) bulk water (experimental) (Murphy, 1977); and (4) gaseous O_3 (experimental) (Andrews, L. & Spiker, 1972); (b) IR emission spectra of (1) $(H_2O)_n$, $10 \leq n \leq 50$; (2) $(H_2O)_{25}$; and (3) $(O_3)_i(H_2O)_{25}$, $1 \leq i \leq 6$ systems and cluster .

The difficulties in studying the Raman spectra $J(\omega)$ of ozone are connected with its high sensitivity to photodecomposition. Nevertheless, in (Andrews & Spiker, 1972), the Raman spectrum of gaseous ozone was obtained with the use of a He–Ne laser at a pressure of 0.2–0.4 MPa. It has been established that the basic $^{16}O_3$ transition frequencies ω_1 and ω_2 are 1103.3 and 702.1 cm^{-1}, respectively, and correspond to individual weak spectral lines shown in Fig. 13(a). The calculated Raman spectra of systems I' and II' and also the Raman

spectrum of bulk water (Murphy, 1977) are illustrated in the same figure. It can be seen that the absorption of ozone leads to an appreciable change in the Raman spectrum of the disperse water system. The integral intensity of the Raman spectrum of system II' consisting of heterogeneous clusters was reduced by 1.8 times. The peaks at 402, 830, and 1016 cm⁻¹ were formed instead of the peaks at 240, 561, and 821 cm⁻¹ in the $J(\omega)$ spectrum of system I'. The main peak of the $J(\omega)$ spectrum reduced its intensity by 1.9 times and had a blue shift from 30 to 65 cm⁻¹. The combination principle consists in that the transitions with the frequencies equal to the combinations (sums or differences) of the frequencies of other transitions can be observed. Taking into account anharmonicity, the weak peak at 830 cm⁻¹ can be considered as an overtone of the peak at 402 cm⁻¹. In the anti-Stokes region of the Raman spectrum of bulk water, the Raman frequency shifts correspond to 53, 143, and 447 cm⁻¹ (Fig. 13(a), curve *3*). The study of a Raman spectrum makes it possible to determine the lifetime of a system in an excited state, or the radiation time τ. After absorbing a photon, a system transfers to a higher energy level, i.e., becoming excited. In the absence of external actions, an excited system loses its energy in the form of emitted photons, so its lifetime is finite. The time τ is reciprocal to the change in the collective vibration frequency (mode difference $\Delta\omega$). To estimate the upper boundary of τ, we choose the minimum $\Delta\omega$ value, which corresponds to the width of the first Raman spectrum peak at half height $\Delta\omega_1$ equal to 71.4 cm⁻¹ for system I' and 133.3 cm⁻¹ for system II'. Hence, the minimum radiation time τ is 0.51 ps for system I' and 0.25 ps for system II'. Therefore, the absorption of ozone molecules by the disperse water system reduces appreciably the observed photon emission time. As the lifetime τ_{cl} of the clusters studied in the given work exceeds the time of computational experiments, i.e., the clusters are not decomposed during the calculations, the radiation time τ of $(O_3)_i(H_2O)_{25}$ clusters, where $1 \le i \le 6$, is at least an order of magnitude less than τ_{cl}.

The radiation source power indicates how quickly the intensity of this radiation is changed. The density of radiation power emitted by the particles determines how clearly these particles are visible. The frequency dependence of the cluster emitted IR radiation power $P(\omega)$ is shown in Fig. 13(b). In system I', the radiation power per cluster (curve *1*) is ~1.3 times higher than the value of P for the $(H_2O)_{25}$ cluster (curve *2*). The $P(\omega)$ spectrum is characterized by a single maximum at 939 cm⁻¹ for system I' and by three maxima at 369, 709, and 956 cm⁻¹ for the $(H_2O)_{25}$ cluster. The scattered IR radiation power is appreciably reduced in the system of $(H_2O)_{25}$ clusters with absorbed ozone molecules (system II'). In this case, the $P(\omega)$ spectrum is also characterized by a single maximum at 942 cm⁻¹. The integral intensity of the emitted radiation power for system II' is 3.4 times lower than that for system I'.

7. Absorption of carbon and nitrogen monoxides by ultradisperse aqueous system

Three systems of clusters were investigated, namely, I'' – a monodisperse system consisting of $(H_2O)_{20}$ clusters, II'' – $(CO)_i(H_2O)_{20}$ clusters, and III'' – $(NO)_i(H_2O)_{20}$ clusters, $i = 1, \dots, 10$. In the frequency range under consideration, the absorptance of IR radiation decreases after absorption of CO molecules by water clusters and increases as a result of absorption of NO molecules by these aggregates (Fig. 14(a)). The integral intensities of IR absorption spectrum for systems I''–III'' are correlated as 1 : 0.71 :1.03. In the case of monodisperse system of $(H_2O)_n$, the $\alpha(\omega)$ spectrum has four peaks at frequencies of 103, 356, 744, and 1023 cm⁻¹. The respective spectrum for systems II'' and III'' is unimodal. For system II'', the peak falls on the
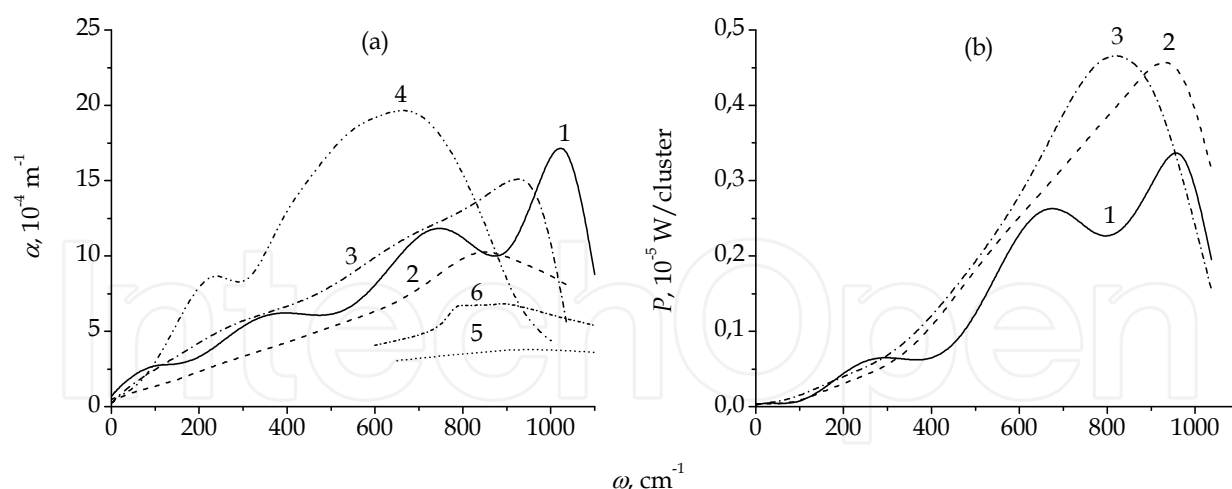
Fig. 14. (a) The absorptance of IR radiation of disperse systems: (*1*) I″, (*2*) II″, (*3*) III″; (*4*) experimentally obtained coefficient α for liquid water (Goggin & Carr, 1986); (*5, 6*) coefficient α of gaseous CO and NO, experiment (Kozintsev et al., 2003); (b) the radiation power generated under conditions of dissipation of thermal energy by systems (*1*) I″, (*2*) II″, (*3*) III″.

frequency of 845 cm⁻¹, and for system III″ – on 925 cm⁻¹. Note that the main peak of $\alpha(\omega)$ spectrum of liquid water falls on the frequency of 690 cm⁻¹ (Goggin & Carr, 1986); for gaseous CO and NO, the extremely slightly pronounced peaks of deformation vibrations correspond to frequencies of 950 and 800 cm⁻¹ (Kozintsev et al., 2003). The weak frequency dependence of the function $\alpha(\omega)$ of gaseous CO and NO shows up in the smoothing of the absorption spectrum of IR radiation for systems II″ and III″ with respect to system I″.

The electromagnetic radiation may be treated as the process of generation of free electromagnetic field under conditions of nonuniform motion and interaction of electric charges. The validity of this approach is supported by the fact that the field of moving electric charge is given by the sum of intrinsic field and field extending to infinitely long distances from the charge. Referred to as intrinsic field is the field which is concentrated in the vicinity of the charge and moves along with this charge. The frequency dependence of the power of radiation of systems I″–III″ is given in Fig. 14(b). The integral power of radiation increases both when the disperse aqueous system absorbs carbon monoxide and when it absorbs nitrogen monoxide. The integral intensities of emission power for systems I″–III″ are correlated as 1 : 1.36 : 1.38. A monodisperse aqueous system has maxima of power of IR radiation on frequencies of 276, 672, and 955 cm⁻¹, and systems II″ and III″—only on frequencies of 930 and 820 cm⁻¹, respectively.

8. Variation of integrated absorption during the growth of clusters

The anti-greenhouse effect can be developed due to a decrease in the number of absorbing centers upon the formation of water clusters. Figure 15(a) (curve 1) shows the relative change in the integrated IR absorption intensity I_{tot} upon the formation of the $(H_2O)_{20}$ cluster by means of successive addition of Δn water molecules to the $(H_2O)_2$ dimer. Curve 2 reflects the total relative intensity of the IR radiation absorption by the $(H_2O)_{10}$ cluster and five successively added dimers, which combine to produce the $(H_2O)_{20}$ cluster.
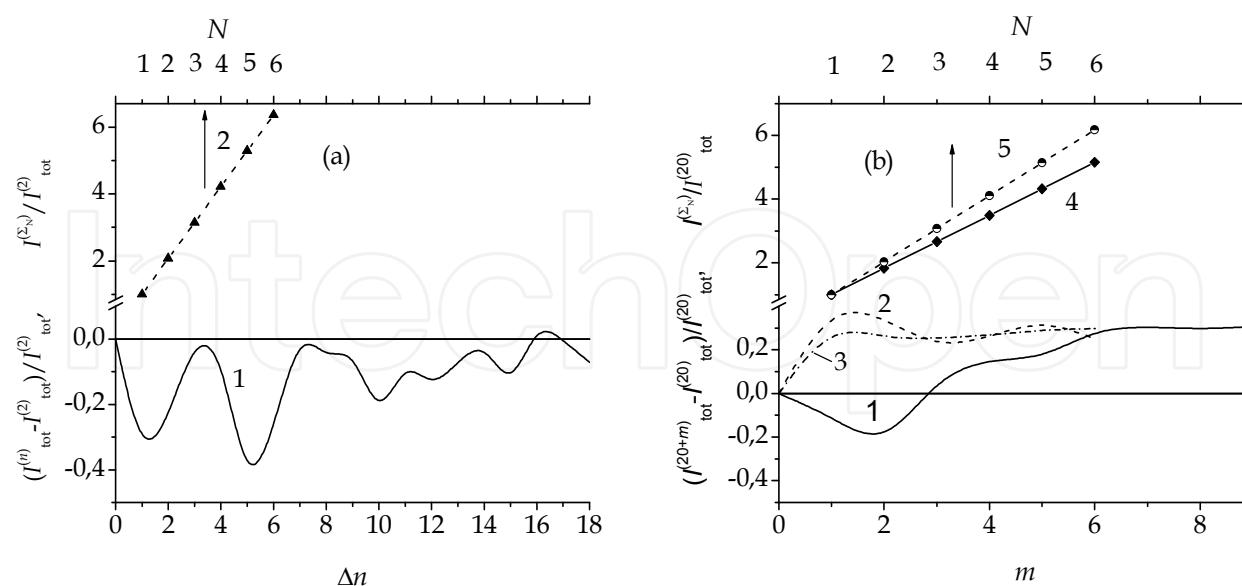
Fig. 15. (a) Relative integrated intensity of the IR absorption by (1) the water dimer that grows by adding Δn H_2O molecules and (2) total relative integrated intensity of absorption of N clusters: N_1 is $(H_2O)_{10}$ and $(N_2–N_6)$ are $(H_2O)_2$ dimers; (b) relative integrated intensity of the IR absorption by the $(H_2O)_{20}$ cluster adding m molecules of (1) CH_4, (2) C_2H_2 and (3) C_2H_6 and total relative integrated intensity of absorption of N clusters: (4) N_1 is $(CH_4)_8(H_2O)_{10}$ and $(N_2–N_6)$ are $(H_2O)_2$ dimers; (5) N_1 is $(CH_4)_3(H_2O)_{10}$ and $(N_2–N_6)$ are $CH_4(H_2O)_2$ clusters.

In the case of water, the formation of the cluster leads to a twofold reduction in the greenhouse effect. The major contribution to the anti-greenhouse effect is made by the decrease in the number of absorbing centers. In addition, the buildup of the water cluster is accompanied by a decrease in its absorption capacity (curve 1 is in the range of negative values almost everywhere) due to a change in the frequency and amplitude characteristics of the total dipole moment. The introduction of hydrocarbon molecules can enhance the IR absorption by growing clusters (Figure 15(b)). The increase in I_{tot} for water cluster combined with C_2H_2 and C_2H_6 molecules is 0.2-0.4 of the I_{tot} value even at $m > 1$, whereas, when water cluster is combined with CH_4 molecules, such I_{tot} values are achieved at m > 6. When one or two CH_4 molecules are added to the $(H_2O)_{20}$ cluster, the anti-greenhouse effect is enhanced since the relative integrated intensity of the IR absorption by the heterocluster decreases. However, finally, the incorporation of hydrocarbon molecules in the water clusters reduces the greenhouse effect due to a decrease in the number of absorbing centers. The anti-greenhouse effect caused by clustering is tens of times stronger than the effect due to a change in the characteristics of vibrations of the total dipole moment of clusters caused by absorption of greenhouse gas molecules.

For estimating the contribution made by the absorption of CO and NO molecules by water clusters, it is important to know the variation of integral absorption during the growth of $X(H_2O)_n$ cluster owing to attachment of X molecules (where X = CO or NO), as well as the integral effect of absorption of IR radiation produced by sets of clusters. In so doing, the combined $X_{10}(H_2O)_n$ cluster is formed of the entire set of clusters.
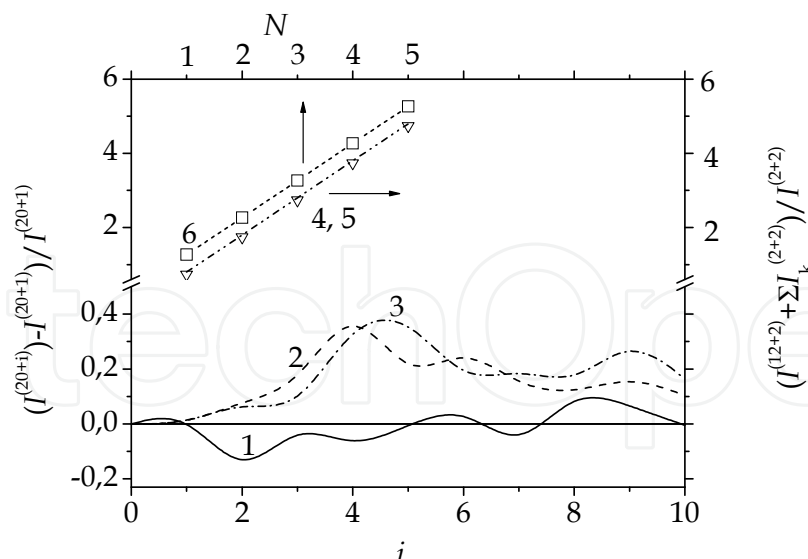
Fig. 16. Relative variation of integral intensity of absorption of IR radiation for clusters: (1) $(H_2O)_{10+i}$, (2) $(CO)_i(H_2O)_{20}$, (3) $(NO)_i(H_2O)_{20}$ as a result of attachment of i molecules of impurity; combined relative intensity of absorption of IR radiation, produced by N clusters: (4) water clusters, (5, 6) clusters of water with CO and NO molecules, respectively.

We will first consider the clustering of water molecules. If water molecules are successively added one-by-one to $(H_2O)_{10}$ cluster, the relative variation of integral intensity of absorption $(I^{(10+i)} - I^{(10)})/ I^{(10)}$ will be defined by curve 1 (Fig. 16). One can see that the quantity under consideration is a sign-variable function of i, i.e., each subsequent, larger, cluster may exhibit both higher and lower integral intensity of IR absorption than $(H_2O)_{10}$ cluster. The integral absorption of the resultant $(H_2O)_{20}$ cluster is 99.5% of IR absorption of the initial $(H_2O)_{10}$ cluster or 92.8% of the value of $I^{(2)}$ for water dimer.

A somewhat different pattern of variation of $(I^{(20+i)} - I^{(20+1)})/ I^{(20+1)}$ is observed in the case of attachment of i X (CO or NO) molecules to $X(H_2O)_{20}$ cluster. In both cases, i.e., where X = CO or NO, the reduced integral intensity of absorption increases relative to the initial value. However, this rise is not monotonic, i.e., each subsequent attachment of X molecule may make the absorptance of cluster both higher and lower than that the cluster had when its size was one X molecule less, if its previous state does not correspond to the initial one. The ratio between the combined values of $(I^{(k+i)} - I^{(k+1)})/ I^{(k+1)}$ (k = 10 for clusters of pure water and k = 20 for clusters of water with CO or NO molecules) for systems I''–III'' is 1 : 20.5 : 20.8. Therefore, the maximal impact on the variation of integral part of absorption of IR radiation caused by the variation of amplitude-frequency characteristics of total dipole moment of cluster is made by the capture of NO molecules by clusters.

We will further consider clusters of three types. Those of the first type are formed by $(H_2O)_{12}$ cluster and successively added $(H_2O)_2$ dimers of water. The dependence of combined intensity of absorption of IR radiation of successive set of clusters on the number of such clusters N is given by points 4. Similarly, $X_2(H_2O)_2$ complexes (miniclusters) were added to the $X_2(H_2O)_{12}$ cluster. In the case of X = CO, the dependence of intensity of absorption of IR radiation of combined cluster on the number N is given by points 5 which coincide with points 4; at X = NO, the analogous function is given by points 6. The relative combined intensity of absorption, given by points 4 and 5, increased by a factor of six as a result of variation of N from 1 to 5, and the analogous characteristic given by points 6 increased by a

factor of four with the same variation of N. The integral intensity of absorption of IR radiation of $(CO)_{10}(H_2O)_{20}$ cluster is 1.16 times lower, and the value of $I^{(20+10)}$ of $(NO)_{10}(H_2O)_{20}$ cluster is 1.18 times that of the similar characteristic for $(CO)_2(H_2O)_2$ and $(NO)_2(H_2O)_2$ complexes, respectively. Of most importance here is the fact that the combined intensity of absorption of initial systems, i.e., of $(H_2O)_{12}$ cluster plus a set of N $(H_2O)_2$ dimers and of $X_2(H_2O)_{12}$ cluster plus a set of N $X_2(H_2O)_2$ complexes, is several times higher than the intensity of absorption of clusters formed of those systems. This effect will be stronger if individual molecules will be attached rather than dimers and complexes. The decrease in combined absorption due to reduction of the number of absorbing centers in the case of molecules uniting into a cluster exceeds many times over the increase in absorption associated with the variation of vibrational characteristics of the total dipole moment. This is the essence of anti-greenhouse effect caused by clustering.

The absorption of IR radiation by a disperse water system insignificantly increases when it incorporates N_2O, C_2H_6, and NO molecules and decreases when CO_2, CH_4, C_2H_2, NO_2, O_3, and CO molecules are incorporated. When methane molecules are incorporated in water clusters, the system becomes IR transparent. Formation of water clusters and subsequent incorporation of greenhouse gases in these clusters are accompanied by a decrease in the number of absorbing centers. Remarkably, the Earth's surface receives on average more radiation from the atmosphere and clouds than direct radiation from the Sun. On the whole, the absorption of greenhouse gases by the disperse water system results in the anti-greenhouse effect. This effect is latent because it can be defined in comparison with situation when clusters are absent. It appears that the same number of free molecules absorbs IR radiation more powerfully than when they are incorporated in a cluster.

The variation of relative combined power of emission upon addition of molecules to clusters is given by Fig. 17. In the case of clusters of pure water, we consider the quantity $(P^{(10+i)} - P^{(10)}) / P^{(10)}$, and for water clusters containing CO or NO molecules—the ratio $(P^{(20+i)} - P^{(20+1)}) / P^{(20+1)}$. Here, P denotes the combined power of IR radiation generated by cluster.

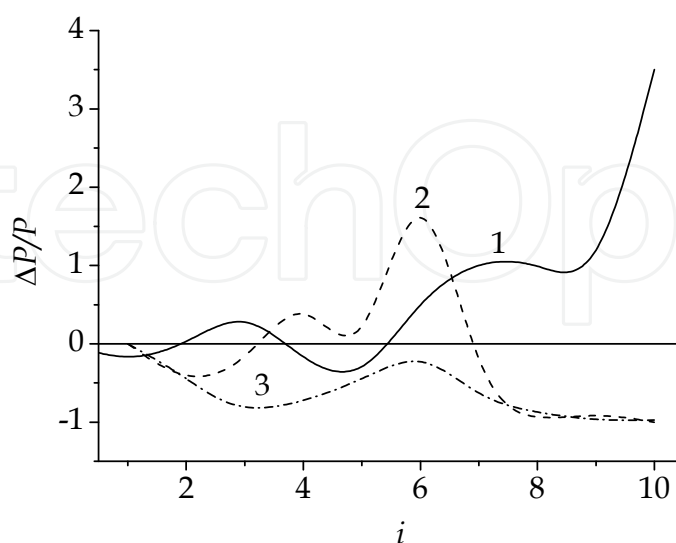Fig. 17. Relative variation of combined intensity of emission of IR radiation for clusters: (1) $(H_2O)_{10+i}$, (2) $(CO)_i(H_2O)_{20}$, (3) $(NO)_i(H_2O)_{20}$ as a result of attachment of i molecules of impurity.

The first term in the superscript indicates the number of water molecules in the cluster, and the second term—the number of molecules of impurity. For clusters of system I'', water molecules are considered instead of molecules of impurity. In all cases, the dependence of relative combined intensity of emission power on the number of molecules i exhibits a fluctuating pattern. For clusters of pure water up to size $n = 16$ ($i = 6$), alternation of decrease and increase in emission power after attachment of individual molecules is observed, i.e., the quantity $(P^{(10+i)} - P^{(10)})/ P^{(10)}$ assumes both negative and positive values. However, at $i >$ 6, this quantity becomes especially positive and rapidly increases in the region of $i \geq 9$. In the case of absorption of CO molecules by clusters, the quantity $(P^{(20+i)} - P^{(20+1)})P^{(20+1)}$ at $i < 7$ may both decrease and increase; at $i \geq 7$, it decreases. When the clusters attach NO molecules, the quantity $(P^{(20+i)} - P^{(20+1)})/P^{(20+1)}$ is always negative at $i > 1$, i.e., the emission power decreases relative to its value corresponding to $NO(H_2O)_{20}$ cluster. Therefore, the power of IR radiation emitted by clusters depends on both the number and the sort of molecules of impurity absorbed by the clusters.

9. Estimation of the greenhouse and anti-greenhouse effect

Atmospheric water clusters absorb IR radiation going from the Earth, as well as free (not incorporated in clusters) molecules of greenhouse gases create a greenhouse effect. However the quantity of absorption by clusters of radiation is not proportional to the number of molecules forming it. Moreover, clusters absorb energy of IR radiation in quantity comparable, and sometimes even smaller, than that absorbed by free water molecule (Fig. 18). As a result free molecules (before they have been incorporated into cluster) make much stronger absorption of IR radiation (the total intensity $\sum I_i$), than clusters (I_{cl}). The difference of values $\sum I_i$ and I_{cl} is defined as an anti-greenhouse effect of the cluster. This value can be expressed in degrees. The estimation of the anti-greenhouse effect that exists now, created by atmospheric water clusters, can be made as follows. The distribution of the atmospheric moisture at altitude submits to the empirical Ghan dependence (Ghan et al., 1997):
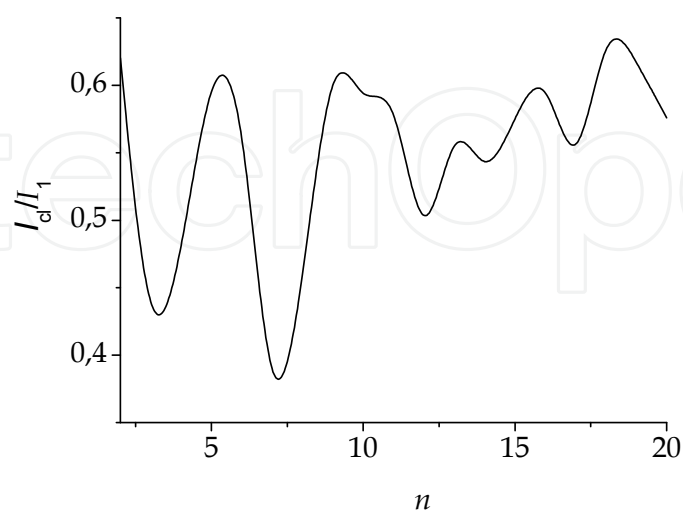

Fig. 18. The relation of integrated intensities of IR radiation absorption by water clusters, formed by n molecules, to the appropriate characteristic of a free water molecule at average surface humidity of 11 g/m^3.

$$\rho = \rho_0 \times 10^{h/6.3} \ , \tag{22}$$

where ρ_0 is the humidity at certain altitude (as a rule, direct at the Earth's surface), h is an altitude in km. On one hand, the formula (22) can be used for calculation of the distribution of water vapor monomer above the Earth's surface, and on another hand – for definition of high-altitude distribution of total moisture in the atmosphere. In the first case, constant ρ_0 is a fraction of water monomers near to the Earth's surface. It can be established by extrapolation of the Boltzmann distribution of clusters on the sizes to the $i = 0$ value. Thus the value determined equals ~ 66.3 % from known value of humidity (~11 g/m³) which at the surface is defined by the number of water monomers and clusters. In the second case value ρ_0 corresponds to the humidity at the altitude of 3 km, established on the basis of spectroscopic measurements (Kebabian et al., 2002). Experimental measurements are executed in the presence of clouds at the altitude from 1 up to 2 km. The spectroscopic sensitive element allows to measure spatially divided profiles of moisture density both around tropospheric clouds, and inside them. Integration on concentric layers of thickness Δh of the first and second distributions gives value of mass M_{vap} of vapor monomers and total quantity M_{tot} of moisture in the atmosphere. The mass of droplets and crystals in the atmosphere was found by the formula

$$M_{drop(cryst)} = \sum_{n=1}^{100} \left(\rho^{(n)} - \rho_{sv}^{(n)} \right) \times V_n \ , \tag{23}$$

where $\rho^{(n)}$ and $\rho_{sv}^{(n)}$ are densities of moisture and saturated water vapor in n layer thickness of 1 km, V_n is the volume of a layer.

We consider particles which size exceeds 0.5 μm (the minimal size of a drop observable in clouds) as drops. Water drops and ice crystals are formed in clouds when T < 273 K, but in the first instance it is necessary for air to be supersaturated in relation to water, and in the second instance it should be supersaturated in relation to ice. Curves of saturation of water vapor taking place above surfaces of water and ice are situated close enough, so both drops and ice crystals can be in the same cloud. Obviously, the full weight of ice in clouds is proportional to concentration of crystal nucleus in clouds. It was accepted, that relative concentration of crystals $c_{crys} = c'_{crys} / (c'_{crys} + c'_{liq})$ linearly changes from 0 to 1 at decrease of temperature from 273 to 230 K (Fletcher, 2011). The mass of ice crystals was determined in accordance with dependence $c_{crys}(T)$ given in Fig. 19. The $\rho_{svl}^{(n)}$ density of saturated water vapor over the supercooled water was designed as $\rho_{sv}^{(n)}$ at the definition of droplets' mass in the atmosphere, and for calculation of crystals' mass the $\rho_{svc}^{(n)}$ density of saturated water vapor over ice at temperature of n layer was used. Masses M_{drop} and M_{cryst} thus were established. The mass of clusters in the atmosphere was defined as

$$M_{cl} = M_{tot} - M_{vap} - M_{drop} - M_{cryst} \ . \tag{24}$$

Similarly, through the appropriate distributions, the high-altitude profile of clusters' density was defined. The designed dependences are given in Fig. 20a. It is visible that the great bulk of water clusters in the atmosphere settles up to an altitude of 2 km. Overwhelming quantity of drops is concentrated within the limits of the same altitude, and crystals are formed, from the altitude of 3 km. The ratio between quantities of monomer vapor, clusters, drops
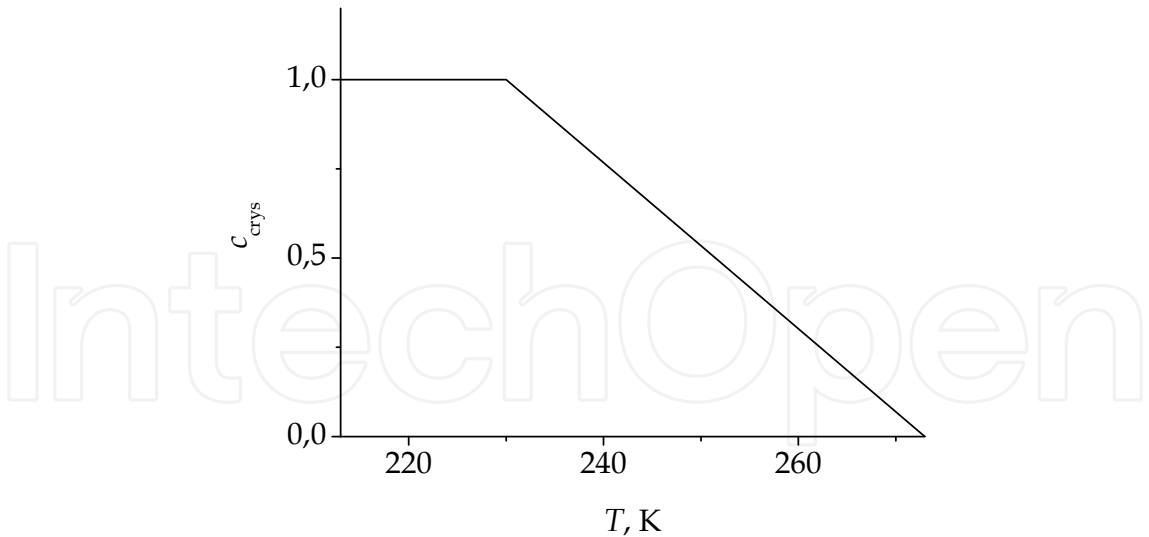
Fig. 19. The fraction of ice crystals in the condensed phase of clouds, determined in accordance with temperature dependences of ice concentration in (Fletcher, 2011).
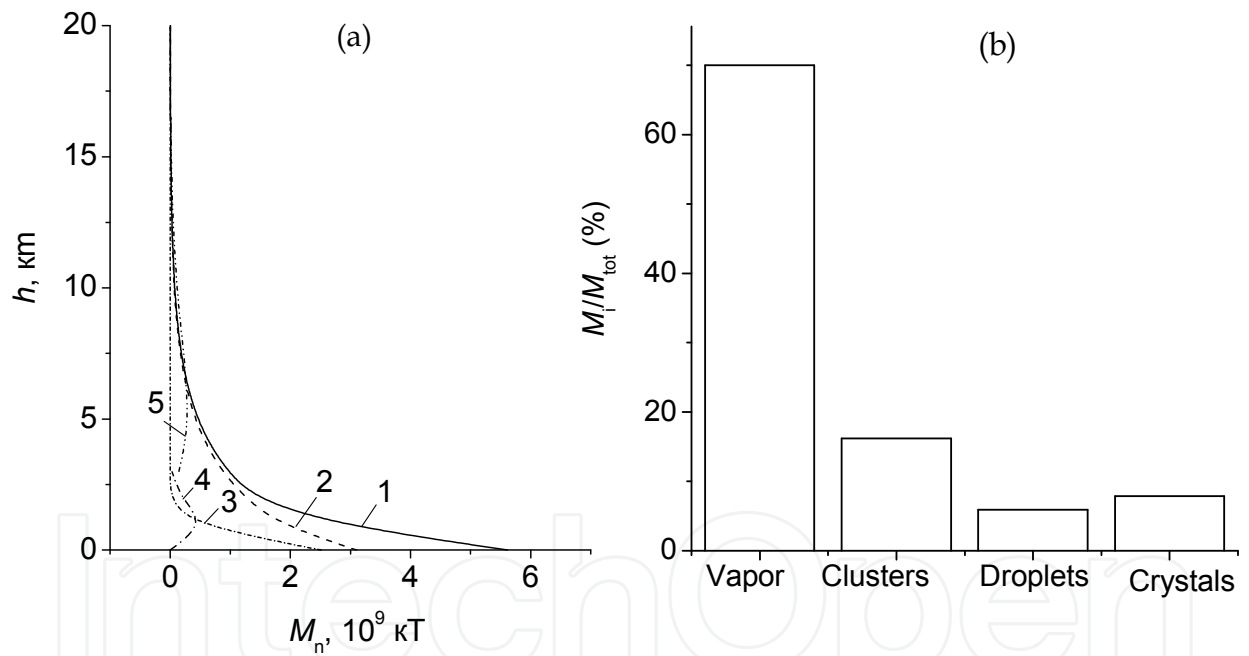

Fig. 20. (a) Contributions to a total mass of the atmosphere moisture: 1 – all moisture, 2 – monomers vapor, 3 – clusters, 4 – droplets, 5 – crystals; (b) the ratio between monomer vapor, clusters, droplets, and crystals, obtained using the linear temperature dependence for the number of crystals in accordance with (Fletcher, 2011).

and crystals looks as 70.0 : 16.2 : 5.9 : 7.9, if total magnitude of the moisture in the atmosphere is 100 % (Fig. 20b). On average, the integrated intensities of IR radiation absorption of water clusters are lower than the intensity of separate molecules. According to the estimation the number of clusters in the atmosphere at time 2.38 is less than the number of molecules forming them. Created by clusters and corresponding free molecules greenhouse effects are ~ 1.0 and 4.3 K accordingly. Thus, the average temperature of the

planet could rise by 4.3-1.0 =3.3 K in the absence of clusters, that would result in a significant change of climate. During the last 100 years the average global temperature of the Earth has gone up by 0.6 K (Halmann & Steinberg, 1999).

10. Conclusion

As the temperature of the atmosphere rises, more water is evaporated from ground storage (rivers, oceans, reservoirs, soil). Because the air is warmer, the absolute humidity can be higher, leading to more water vapor in the atmosphere. In other words, the air is able to "hold" more water when it's warmer. As a greenhouse gas, the higher concentration of water vapor is then able to absorb more thermal IR energy radiated from the Earth, thus further warming the atmosphere. The warmer atmosphere can then hold more water vapor and so on. However as water vapor increases in the atmosphere, more of it will eventually also condense into clouds, which are more able to reflect incoming solar radiation and thus allowing less energy to reach the Earth's surface and heat it up.

Besides water vapor, many other feedback mechanisms operate in the Earth's climate system and impact the sensitivity of the climate response to an applied radiative forcing. The relative strengths of feedback interactions between clouds, aerosols, snow, ice, and vegetation, including the effects of energy exchange between the atmosphere and ocean, create a great influence on climate. For the greenhouse effect to work efficiently, the Earth's atmosphere must be relatively transparent to sunlight at visible wavelengths so that significant amounts of solar radiation can penetrate to the ground. Also, the atmosphere must be opaque at thermal wavelengths to prevent thermal radiation emitted by the ground from escaping directly to space. Without the presence of water vapor, carbon dioxide, and other gases in the atmosphere, too much heat would escape and the Earth would be too cold to sustain life. Carbon dioxide, methane, nitrous oxide, and other greenhouse gases absorb the infrared radiation rising from the Earth and hold this heat in the atmosphere instead of reflecting it back into space. Although greenhouse gases make up only about 1 percent of the Earth's atmosphere, they regulate our climate by trapping heat and holding it in a kind of warm-air blanket that surrounds the planet.

Until recently there is no complete picture of all the factors influencing climate change. The reliability of forecasts depends on an understanding of cycles that result in climate change. In the present work we have shown that atmospheric water clusters are also capable of influencing the climate. Accumulation of CO_2 in the atmosphere has increased since 1900. By 2000 the volumetric concentration of CO_2 has increased by 1.25 times. The anti-greenhouse effect created by clusterization of the atmospheric water vapor limits the growth of global temperature.

When water evaporates from the surface of the Earth, it cools the surface. This keeps the surface from getting too hot. The total cooling effect of water evaporation from the surface of seas and reservoirs, is 13.4 K. Transition of the part of atmospheric water vapor into clusters causes a decrease of atmospheric temperature by 3.3 K, that is the effect of 24.6% cooling of the heat received during water evaporation. The thermal energy of the lower atmosphere reaches the upper atmosphere by radiative transfer, thermal conduction, convection and by the release of energy when water vapor condenses. From the higher atmosphere radiative transfer becomes overwhelmingly predominant as the loss of energy to space can only take place radiatively. The potential absorption by the combination of water vapor and CO_2 is almost complete due to the logarithmic relationship between

concentration and radiance/absorption. Thus, the content of CO_2 in the atmosphere of the Earth is not an absolute criterion of the efficiency of the greenhouse effect made by this gas which now is estimated at 9.3 K, i.e. constitutes about 19.6% of the effect given by all greenhouse gases. In the absence of reliable thermal protection from the ozone layer of the lower stratosphere and depletion of atomic oxygen in the thermosphere, CO_2 can partially or completely carry out the functions of anti-greenhouse gas.

The bulk of clusters are concentrated up to the altitude of 2 km, and the droplets are largely located at altitudes up to 2.5 km. The crystals are, as a rule, located above 3 km. Water vapor is most widespread among other components of atmospheric moisture. Water clusters are injected into the upper atmosphere during flights of space vehicles. Such clusters may exist for a long time; however, their fraction is small at present, and the greenhouse effect they produce is low.

It is well known that condensed phase reactions occurring in the Earth's atmosphere play a role in atmospheric phenomena, for example, in the formation of the Antarctic ozone hole. The presence of the XH_2O complexes (X is a molecule of greenhouse gases) in the Earth's atmosphere is confirmed both experimentally and theoretically. Weakly bound complexes, considered as precursors to the condensed phase, are important because perturbations and interactions between the monomer units can alter the spectroscopy and reactivity compared with the constituent molecules. Water is a major component in the absorption of radiation in the atmosphere and is a key component in the Earth's radiative balance. The significant abundances of H_2O and high absorbability of greenhouse gases (including water) in the atmosphere could affect the Earth's climate.

Water vapour is itself too strong a greenhouse gas. However the greenhouse effect will decrease at presence of the clusters formation in water vapour instead of to amplify. The increase of the water vapour content in atmosphere at the present condition of an atmosphere results in amplification of a greenhouse effect, but not in direct ratio to quantity added vapour. Now clusters are formed and they reduce a greenhouse effect. However there can come the moment of such warming in atmosphere, that clusters will not be formed. It will result to significant jump of global temperature and its further very fast growth, i.e. to catastrophe.

Clouds modulate Earth's radiation and water balances, namely:

clouds cool Earth's surface by reflecting incoming sunlight;

clouds warm Earth's surface by absorbing heat emitted from the surface and re-radiating it back down toward the surface; clouds warm or cool Earth's atmosphere by absorbing heat emitted from the surface and radiating it to space; clouds warm and dry Earth's atmosphere and supply water to the surface by forming precipitation;

clouds are themselves created by the motions of the atmosphere that are caused by the warming or cooling of radiation and precipitation.

If the climate should change, then clouds would also change, altering all of the effects mentioned above. What is important is the sum of all these separate effects, the net radiative cooling or warming effect of all clouds on Earth. If Earth's climate should warm due to the greenhouse effect , the weather patterns and the associated clouds would change. However it is not known whether the resulting cloud changes would diminish the warming (a negative feedback) or enhance the warming (a positive feedback). Moreover, it is not known whether these cloud changes would involve increased or decreased precipitation and water supplies in particular regions. Improving our understanding of the role of clouds in climate is crucial to understanding the effects of global warming.

11. References

Agmon, N. (1996) Tetrahedral Displacement: The Molecular Mechanism behind the Debye Relaxation in Water. *Journal of Physical Chemistry*, Vol. 100, No.3, pp. 1072–1080, ISSN 0022–3654.

Akhmatskaya, E.V.; Apps, C.J.; Hillier, I.H.; Masters, A.J.; Watt, N.E. & Whitehead, J.C. Formation of H_2SO_4 from SO_3 and H_2O, Catalysed in Water Clusters. *Chemical Communications*, 1997, Issue 7, pp. 707–708, ISSN 1364–548X.

Allouch, A. (1999) Quantum Study of Acetylene Adsorption on Ice Surface. *Journal of Physical Chemistry A*, Vol. 103, No.45, pp. 9150–9153, ISSN 1538–6414.

Andrews, L. & Spiker, R.C. (1972) Argon Matrix Raman and Infrared Spectra and Vibrational Analysis of Ozone and the Oxygen_18 Substituted Ozone Molecules. *Journal of Physical Chemistry*, Vol. 76, No. 22, pp. 3208–3213, ISSN 0022–3654.

Barrett, J. (2005) Greenhouse Molecules, Their Spectra and Function in the Atmosphere. *Energy & Environment,* Vol.16, No.6, pp. 1037-1045, ISSN 0958–305X.

Benedict, W.S.; Gailar, N. & Plyler, E.K. (1956) Rotation–Vibration Spectra of Deuterated Water Vapor. *Journal of Chemical Physics,* Vol.24. No.6, pp. 1139-1165, ISSN 0021–9606.

Bignell, J. (1970) The Water Vapour Infrared Continuum. *Quarterly Journal of the Royal Meteorological Society*, Vol.96, Issue 409, 390–403, ISSN 1477–870X.

Bosma, W.B.; Fried, L.E. & Mukamel, S.J. (1993) Simulation of the Intermolecular Vibrational Spectra of Liquid Water and Water Clusters, *Journal of Chemical Physics*, Vol.98, No.6, pp. 4413-4421.

Bresme, F. (2001) Equilibrium and Nonequilibrium Molecular-Dynamics of the Central Force Model of Water. *Journal of Chemical Physics*, V.115, No. 16, pp. 7564–7574, ISSN 0021–9606.

Carlon, H.R. (1979) Do Clusters Contribute to the Infrared Absorption Spectrum of Water Vapor? *Infrared Physics,* Vol.19, No.5, pp. 549–557, ISSN: 0020-0891.

Chukanov, V. N. & Galashev, A. Y. (2008) Cluster Mechanism of the Anti-Greenhouse Effect. *Doklady Physical Chemistry*, Vol.421, Part 2, pp. 226–229, ISSN 0012-5016.

Coffey, M.T. (1977) Water Vapour Absorption in 10-12 μm Atmospheric Window. *Quarterly Journal of the Royal Meteorological Society*, Vol.103, Issue 438, pp. 685–692, ISSN 1477–870X.

Dang, L.X. & Chang, T.M. (1997) Molecular Dynamics Study of Water Clusters, Liquid and Liquid–Vapor Interface of Water with Many-Body Potentials. *Journal of Chemical Physics*, Vol.106, No.19, pp. 8149-8159, ISSN 0021–9606.

Dias-Lalcaca, P.; Packham N.J.C. & Gebbie H.A. (1981) The Effect of Ultraviolet Radiation on Water Vapour Absorption Between 5 and $50cm^{-1}$. *Infrared Physics*, Vol.24, No.5, pp. 437-441, ISSN: 0020-0891.

Essenhigh, R.H. (2009) Potential Dependence of Global Warming on the Residence Time (RT) in the Atmosphere of Anthropogenically Sourced Carbon Dioxide. Energy & *Fuels*, Vol. 23, No.5, pp. 2773–2784, ISSN: 0887-0624.

Feller, D. & Dixon, D.A. (1996) The Hydrogen Bond Energy of the Trimer. *Journal of Physical Chemistry*, Vol.100, No.8, pp. 2993–2997, ISSN 0022-3654.

Fichet, P., Jevais, J.R., Camy-Peyret, C. & Flaud, J.M. (1992) Calculation of NLTE Ozone Infrared Spectra, *Planetary Space Science*, Vol. 40, No.9, p. 1289–1297, ISSN 0032–0633.

Fletcher, N.H. (2011) *The Physics of Rainclouds*. University Press, ISBN-13:9780521154796, Cambridge, UK.

Frish, M.J.; Pople, J.P. & Del Bene, J.E. (1983) Hydrogen Bonds Between First-Row Hydrides and Acetylene. *Journal of Chemical Physics*, Vol.78, No.6, pp. 4063–4065, ISSN 0021–9606.

Galashev, A.Y.; Rakhmanova, O.R. & Chukanov, V.N. (2005) Absorption and Dissipation of Infrared Radiation by Atmospheric Water Clusters, *Russian Journal of Physical Chemistry A,* Vol.79, No.9, pp. 1455-1159, ISSN 0036–0244.

Galashev, A. Y.; Chukanov, V. N.; Novruzov, A. N. & Novruzova, O. A. (2006a) Molecular-Dynamic Calculation of Spectral Characteristics of Absorption of Infrared Radiation by $(H_2O)_j$ and $(CH_4)_i(H_2O)_n$ Clusters. *High Temperature*, Vol. 44, No.3, pp. 364–372, ISSN 0018–151X.

Galashev, A. Y.; Rakhmanova, O. R.; Galasheva, O. A. & Novruzov, A. N. (2006b) Molecular Dynamics Study of the Greenhouse Gases Clusterization. *Phase Transitions*, Vol.79, No.11, pp. 911–920, ISSN 0141-1594.

Galashev, A. Y.; Chukanov, V. N.; Novruzov, A. N. & Novruzova, O. A. (2007) Simulation of Dielectric Properties and Stability of Clusters $(H_2O)_i$, $CO_2(H_2O)_i$, and $CH_4(H_2O)_i$. *Russian Journal of Electrochemistry*, Vol.43, No.2, pp. 136–145, ISSN 1023–1935.

Galashev, A. Y. (2011) Greenhouse Effect of Clusterization of CO_2 and CH_4 with Atmospheric Moisture. *Environmental Chemistry Letters*, Vol.9, No.1, pp. 37–41, ISSN 1610-3653.

Galasheva, A. A.; Rakhmanova, O. R.; Novruzov, A. N. & Galashev, A. Y. (2007) Spectral Effects of the Clusterization of Greenhouse Gases: Computer Experiment. *Colloid Journal*, Vol.69, No.1, pp. 56–65, ISSN 1061–933X.

Gear, C.W. (1971) The Automatic Integration of Ordinary Differential Equations, *Communications of the* ACM, Vol.14, Issue 3, pp. 176-179, ISSN 0001–0782.

Ghan, S.J.; Leung, L.R.; Easter, R.C. & Abdul-Razzak, H. (1997) Prediction of Cloud Droplet Number in a General Circulation Model, *Journal of Geophysical Research,* Vol.102, D18, pp. 777–794, ISSN 0148–0227.

Goggin, P.L. & Carr, C. (1986) Far Infrared Spectroscopy and Aqueous Solutions, In: *Water and Aqueous Solutions,* Vol. 37, G.W. Neilson & J.E. Enderby, (Ed.), 149-161, Adam Hilger, ISBN 0-85274–576–1, Bristol, USA.

Goss, L.M.; Sharpe, S.W.; Blake, T.A.; Vaida, V. & Brault, J.W. (1999) Direct Absorption Spectroscopy of Water Clusters. *Journal of Physical Chemistry A 103*, No.43, 1999, 8620–8624, ISSN 1538–6414.

Günzler, H. & Gremlich, H.-U. (2002) *IR Spectroscopy. An Introduction*, Wiley-VCH, ISBN 3–527–28896–1, Weinheim, Germany.

Halle, B. & Karlstrom, G. (1983) Prototropic Charge Migration in Water. Part 1.—Rate Constants in Light and Heavy Water and in Salt Solution from Oxygen-17 Spin Relaxation. *Journal of the Chemical Society, Faraday Transactions*, Vol. 79, No.7, pp. 1031–1046, ISSN 0956–5000.

Halmann, M.M. & Steinberg, M. (1999) *Greenhouse Gas Carbon Dioxide Mitigation. Science and Technology*, Lewis publishers, ISBN 1–56670-284–4, Roca Raton, London, New York, Washington, USA.

Jorgensen, W.L. (1981) Transferable Intermolecular Potential Functions for Water, Alcohols and Ethers. Application to Liquid Water. *Journal of American Chemical Society*, Vol.103. No.2, pp. 335-340, ISSN 0002–7863.

Kebabian, P.L.; Kolb, C.E. & Freedman, A. (2002) Spectroscopic Water Vapor Sensor for Rapid Response Measurements of Humidity in the Troposphere. *Journal of Geophysical Research*, Vol.107, D23, 4670, 14 pp, ISSN 0148-0227.

Kirov, M.V. (1993) F-structure of polyhedral water clusters, *Journal of Structural Chemistry*, Vol. 34, No. 4, pp. 557-561, ISSN 0022–4766.

Kozintsev, V.I.; Belov, M.L.; Gorodnichev, V.A. & Fedotov, Yu.V. (2003) *Lazernyi Optiko-Akusticheskii Analiz Mnogokomponentnykh Gazovykh Smesei [Laser Optical Acoustic Analysis of Multicomponent Gas Mixtures]*, Izd. MGTU im. N.E. Baumana, ISBN 5–7038–2134–7, Moscow, Russia.

Landau, L.D. & Lifshits E. M. (2001) *Elektrodinamika Sploshnykh Sred [Electrodynamics of Continuous Media]*, Vol. 8, Fizmatlit, ISBN 5–9221–0125–0, Moscow, Russia.

Lee, A.C.L. (1973) A Study of the Continuum Absorption Within the 8-13 μm Atmospheric Window. *Quarterly Journal of the Royal Meteorological Society*. Vol.99, Issue 421, pp. 490–505, ISSN 1477–870X.

Levanuk, A.P. & Sannikov, D.G. (1988) Dielectric Loses, In: *Fizicheskaya Entsiklopediya [Physical Encyclopedia]*, Vol. 1, A.M. Prokhorov, (Ed.), 702, Sovetskaya Entsiklopediya, ISBN 5–85270–034–7, Moscow, USSR.

Lide D.R. (Ed.) (1996) *CRC Handbook of Chemistry and Physics*. 77th edition, CRC Press, ISBN-13: 978-0849304774, Boca Ration-New York-London-Tokyo, USA.

Maheshwary, S.; Patel, N.; Sathyamurthy, N.; Kulkarni, A.D. & Gadre, S.R. (2001) Structure and Stability of Water Clusters $(H_2O)_n$, n=8–20: An Ab initio Investigation. *Journal of Physical Chemistry A*, Vol.105, No.46, pp. 10525–10537, ISSN 1538–6414.

Murphy, W.F. (1977) The Rayleigh Depolarization Ratio and Rotational Raman Spectrum of Water Vapor and the Polarizability Components for the Water Molecule, *Journal of Chemical Physics*, Vol. 67, No.12, pp. 5877– 5882, ISSN 0021–9606.

Neumann, M. (1985) The Dielectric Constant of Water. Computer Simulations with the MCY Potential, *Journal of Chemical Physics*, Vol.82, No.12, pp. 5663-5672, ISSN 0021–9606.

Neumann, M. (1986) Dielectric Relaxation in Water. Computer Simulations with the TIP4P Potential. *Journal of Chemical Physics*, Vol. 85, No. 3, pp. 1567–1679, ISSN 0021–9606.

Novruzov, A. N.; Chukanov, V. N.; Rakhmanova O. R. & Galashev, A. Y. (2006) A Computer Study of the Absorption of Infrared Radiation by Systems of Molecular Clusters. *High Temperature*, Vol.44, No.6, pp. 932–940, ISSN 0018–151X.

Novruzov, A.N.; Rakhmanova, O.R.; Novruzova, O.A. & Galashev, A.Y. (2008a) The Structure of Water Clusters Interacting with Gaseous Acetylene. *Russian Journal of Physical Chemistry B*, Vol. 2, No. 1, pp. 115–122, ISSN 1990-7931.

Novruzov, A.N.; Rakhmanova, O.R. & Galashev, A.Y. (2008b) Computer Simulation of the Structure of Water Clusters Containing Absorbed Ethane Molecules. *Colloid Journal*, Vol. 70, No. 1, pp. 64–70, ISSN 1061–933X.

Novruzova, O.A.; Galasheva, A.A. & Galashev, A.Y. (2007a) IR Spectra of Aqueous Disperse Systems Adsorbed Atmospheric Gases: 1. Nitrogen. *Colloid Journal*, Vol.69, No.4, pp. 474-482, ISSN 1061–933X.

Novruzova, O.A.; Galasheva, A.A. & Galashev, A.Y. (2007b) IR Spectra of Aqueous Disperse Systems Adsorbed Atmospheric Gases: 2. Argon. *Colloid Journal*, Vol.69, No.4, pp. 483-491, ISSN 1061–933X.

Novruzova, O.A. & Galashev, A.Y. (2008) Numerical Simulation of IR Absorption, Reflection, and Scattering in Dispersed Water-Oxigen Media. *High Temperature.* Vol.46, No.1, pp. 60-68, ISSN 0018–151X.

Petrov, K.G. & Tikhonov A.A. (2002) Equations of rotary motion of a rigid body based on the utilization of quaternion parameters. Mechanics of solid, Vol.37, No.3, pp. 1–12, ISSN 0025–6544.

Platt, U. & Stutz, J. (2008) *Differential Optical Absorption Spectroscopy. Principles and Applications*. Springer, ISBN 978-3-540-21193-8, Verlag-berlin-Heidelberg, Germany.

Poulet, H.& Mathieu, J.-P. (1970) *Specters de Vibration et Symetrie des Cristaux*, Gordon & Breach, ISBN 0677501803, New York, USA.

Przhibel'sky S.G. (1994) The molecular scattering of light, In: *Fizicheskaya Entsiklopediya [Physical Encyclopedia]*, Vol. 4, A.M. Prokhorov, (Ed.), 280–283, Sovetskaya Entsiklopediya, ISBN5–85270–087–8, Moscow, Russia.

Shillings, A. J. L.; Ball, S. M.; Barber, M. J.; Tennyson, J. & Jones R. L. (2010) A Upper Limit for Water Dimer Absorption in the 750nm Spectral Region and a Revised Water Line List. *Atmospheric Chemistry and Physics Discussions*, Vol.10, No.5, pp. 23345–23380, ISSN 1680–7316.

Silva, S.C. & Devlin, J.P. (1994) Interaction of Acetylene, Ethylene, and Benzene with Ice Surfaces. *Journal of Physical Chemistry*, Vol.98, No.42, pp. 10847–10852, ISSN 0022-3654.

Smith, D.E. & Dang, L.X. (1994) Simulations of NaCl Association in Polarizable Water. *Journal of Chemical Physics*, Vol.100, No.5, pp. 3757–3762, ISSN 0021–9606.

Sonnenschein, R. (1985) An Improved Algorithm for Molecular Dynamics Simulation of Rigid Molecules. *Journal of Computational Physics,* Vol.59, No.2, pp. 347–350, ISSN 0021–9991.

Spackman, M.A. (1986a) Atom-Atom Potentials via Electron Gas Theory. *Journal of Chemical Physics*, Vol.85, No.11, pp. 6579–6585, ISSN 0021–9606.

Spackman, M.A. (1986b) A Simple Quantitative Model of Hydrogen Bonding. *Journal of Chemical Physics*, Vol.85, No.11, pp. 6587–6601, ISSN 0021–9606.

Sremaniak, L.S.; Perera, L. & Berkowitz, M.L. (1996) Cube to Cage Transitions in $(H_2O)_n$ (n=12, 16, and 20), *Journal of Chemical Physics*, Vol.105, No.9, pp. 3715–3721, ISSN 0021–9606.

Stern, H.A. & Berne, B.J. (2001) Quantum Effects in Liquid Water: Pathintegral Simulations of a Flexible and Polarizable Ab initio Model. *Journal of Chemical Physics*, Vol.115, No.16, pp. 7622–7628, ISSN 0021–9606.

Tsai C.J. & Jordan, K.D. (1993) Theoretical Study of Small Water Clusters: Low-Energy Fused Cubic Structures for $(H_2O)_n$, n=8, 12, 16, and 20. *Journal of Physical Chemistry*, Vol.97, No. 20, pp. 5208–5210, ISSN 0022–3654.

Vaida, V.; Daniels, J.S.; Kjaergaard, H.G.; Goss, L.M. & Tuck, A.F. (2001) Atmospheric Absorption of Near Infrared and Visible Solar Radiation by the Hydrogen Bonded Water Dimmer, *Quarterly Journal of the Royal Meteorological Society*, Vol.127, Issue 575, pp. 1627–1643, ISSN 1477–870X.

Wales, D.J. & Ohmine, I. (1993) Structure, Dynamics, and Thermodynamics of Model $(H_2O)_8$ and $(H_2O)_{20}$ Clusters. *Journal of Chemical Physics*, Vol.98, No.9, pp. 7245–7256, ISSN 0021–9606.

Wilson, E.B.Jr.; Decius, J.C. & Cross, P.C. (1980) *Molecular Vibrations. The Theory of Infrared and Raman Vibrational Spectra*, Dover Publications, ISBN 0–486–63941–X, New York, USA.

Wolynes, P.G. & Roberts, R.E. (1978) Molecular Interpretation of the Infrared Water Vapour Continuum. *Applied Optics,* Vol.17, No.10, pp. 1484–1485, ISSN 0003–6935.

Xantheas, S. (1996) The Hamiltonian for a Weakly Interacting Trimer of Polyatomic Monomers. *Journal of Chemical Physics,* Vol.104. No.21. pp. 8821–8824, ISSN 0021–9606.

Xie, F.; Tian, W. & Chipperfield, M.P. (2008) Radiative Effect of Ozone Change on Stratosphere-Troposphere Exchange. *Journal of Geophysical Research*, Vol.113, D00B09, 15 pp., ISSN 0148–0227.
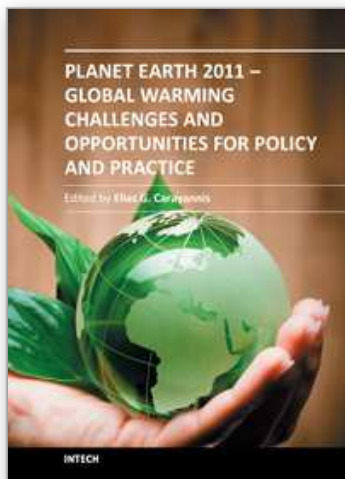
Planet Earth 2011 - Global Warming Challenges and Opportunities for Policy and Practice

Edited by Prof. Elias Carayannis

The failure of the UN climate change summit in Copenhagen in December 2009 to effectively reach a global agreement on emission reduction targets, led many within the developing world to view this as a reversal of the Kyoto Protocol and an attempt by the developed nations to shirk out of their responsibility for climate change. The issue of global warming has been at the top of the political agenda for a number of years and has become even more pressing with the rapid industrialization taking place in China and India. This book looks at the effects of climate change throughout different regions of the world and discusses to what extent cleantech and environmental initiatives such as the destruction of fluorinated greenhouse gases, biofuels, and the role of plant breeding and biotechnology. The book concludes with an insight into the socio-religious impact that global warming has, citing Christianity and Islam.

How to reference

In order to correctly reference this scholarly work, feel free to copy and paste the following:

Alexander Y. Galashev (2011). Climatic Effect of the Greenhouse Gases Clusterization, Planet Earth 2011 - Global Warming Challenges and Opportunities for Policy and Practice, Prof. Elias Carayannis (Ed.), ISBN: 978-953-307-733-8, InTech, Available from: http://www.intechopen.com/books/planet-earth-2011-global-warming-challenges-and-opportunities-for-policy-and-practice/climatic-effect-of-the-greenhouse-gases-clusterization

INTECH
open science | open minds